ACS Pharmacology & Translational Science

pubs.acs.org/ptsci
Article

Diastereomers of Coibamide A Show Altered Sec61 Client Selectivity and Ligand-Dependent Activity against Patient-Derived Glioma Stem-like Cells

Daphne R. Mattos, Willian das Neves, Takashi Kitamura, Richa Pradhan, Xuemei Wan, Cintia Carla da Hora, Dale Tranter, Soheila Kazemi, Xinhui Yu, Nirmalya Tripathy, Ville O. Paavilainen, Kerry L. McPhail, Shinya Oishi, Christian E. Badr,* and Jane E. Ishmael*

Cite This: *ACS Pharmacol. Transl. Sci.* 2024, 7, 1823−1838

Read Online

ACCESS | Metrics & More | Article Recommendations | Supporting Information

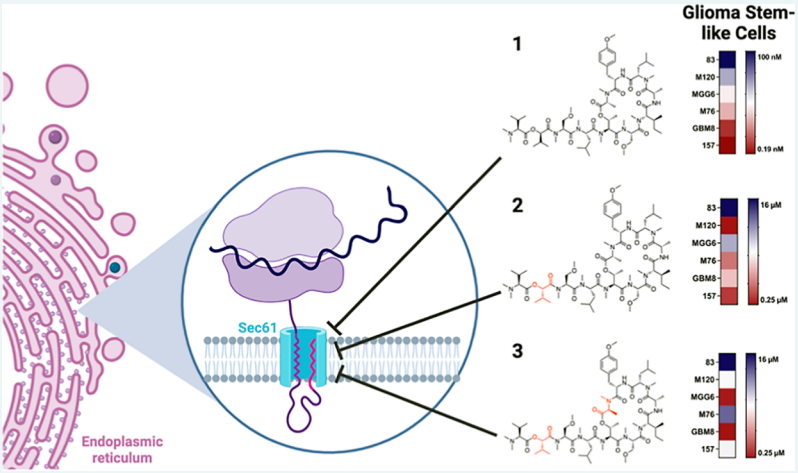

ABSTRACT: Coibamide A (CbA) is a cyanobacterial lariat depsipeptide that selectively inhibits multiple secreted and integral membrane proteins from entering the endoplasmic reticulum secretory pathway through binding the alpha subunit of the Sec61 translocon. As a complex peptide-based macrocycle with 13 stereogenic centers, CbA is presumed to adopt a conformationally restricted orientation in the ligand-bound state, resulting in potent antitumor and antiangiogenic bioactivity. A stereochemical structure−activity relationship for CbA was previously defined based on cytotoxicity against established cancer cell lines. However, the ability of synthetic isomers to inhibit the biosynthesis of specific Sec61 substrates was unknown. Here, we report that two less toxic diastereomers of CbA, [L-Hiv^{2}]-CbA and [L-Hiv^{2}, L-MeAla^{11}]-CbA, are pharmacologically active Sec61 inhibitors. Both compounds inhibited the expression of a secreted reporter (*Gaussia* luciferase), VEGF-A, and a Type 1 membrane protein (VCAM1), while [L-Hiv^{2}]-CbA also decreased the expression of ICAM1 and BiP/GRP78. Analysis of 43 different chemokines in the secretome of SF-268 glioblastoma cells revealed different inhibitory profiles for the two diastereomers. When the cytotoxic potential of CbA compounds was compared against a panel of patient-derived glioblastoma stem-like cells (GSCs), Sec61 inhibitors were remarkably toxic to five of the six GSCs tested. Each ligand showed a distinct cytotoxic potency and selectivity pattern for CbA-sensitive GSCs, with IC_{50} values ranging from subnanomolar to low micromolar concentrations. Together, these findings highlight the extreme sensitivity of GSCs to Sec61 modulation and the importance of ligand stereochemistry in determining the spectrum of inhibited Sec61 client proteins.

KEYWORDS: *coibamide A, GSCs, macrocyclic peptide, Sec61, secretome, translocon*

Coibamide A (CbA, **1**) is a cytotoxic lariat depsipeptide produced by an assemblage of filamentous cyanobacteria in the Coiba National Park, Panama, and one of several natural product inhibitors of Sec61.[1−3] The Sec61 translocon is a highly conserved protein-conducting channel that facilitates the initial insertion of most secreted and integral membrane proteins into the early protein secretion pathway.[4,5] Nascent

Received: January 30, 2024
Revised: April 23, 2024
Accepted: April 29, 2024
Published: May 14, 2024

https://doi.org/10.1021/acsptsci.4c00049
ACS Pharmacol. Transl. Sci. 2024, 7, 1823−1838

polypeptides, destined for the secretory pathway are guided to the rough endoplasmic reticulum (ER) in the context of a ribosome-nascent chain complex (RNC) when specific targeting sequences, such as an N-terminal signal peptide (SP), or transmembrane segment, are recognized by a signal recognition particle (SRP).[6−8] Cytosolic SRP-RNCs move to the ER membrane through interaction with the SRP receptor and are subsequently transferred to the Sec61 channel complex where the nascent polypeptide is cotranslationally translocated either into the ER lumen or inserted into the ER membrane.[5−9] The core Sec61 translocon comprises a central, pore-forming alpha subunit and smaller beta and gamma subunits.[10,11] Structural models support the specialized functional requirements of this channel and have revealed an elaborate arrangement by which nascent proteins are funneled into the ER lumen or exit laterally into the ER membrane via luminal, or lateral gates of the α subunit, respectively.[12,13] Through interactions with numerous accessory proteins and cofactors, the Sec61 channel complex signals with the downstream protein folding machinery of the ER lumen, such as BiP, as well as upstream with the cytoplasmic protein translocation machinery.[13,14]

At least six natural products are known to specifically bind Sec61 and inhibit protein import into the ER.[2,3,14−18] These specialized metabolites are produced by a diverse range of marine and terrestrial organisms yet, as a mechanistic set, interact with a similar region of the Sec61α subunit at the ER luminal side of the channel.[3,17−21] The potential for pharmacological manipulation of Sec61 function was first demonstrated when modifications to the chemical structure of a fungal natural product inhibitor of cell adhesion, HUN-7293, resulted in the generation of synthetic cotransins with greater selectivity and potency for specific Sec61 substrates.[15,16,22−25] The selectivity with which cotransin-like molecules, including a natural analogue of HUN-7293 (CAM741), and a synthetic molecule cyclotriazadisulfonamide (CADA), reversibly block the biosynthesis of a subset of secretory pathway proteins was found to be dependent on the ER targeting sequence of the Sec61 substrate and the ligand concentration.[15,16,25−28] Over time, a more complete understanding of this mechanism has formed the basis for the current pharmacologic classification of Sec61 inhibitors that distinguishes the substrate-selective inhibitors, acting at the level of the SP, from the broad-spectrum inhibitors.[3,14] Recent structural models of ligand-bound human Sec61 complexes obtained using cryogenic electron microscopy (cryo-EM) continue to support and extend a critical role for the SP as the basis for Sec61 substrate selectivity.[12,18] For example, promising selectivity has recently been achieved for a nontoxic cotransin-like molecule, KZR-8445, that discriminates between pro-inflammatory cytokines in a SP-dependent manner.[12] Cytokines, such as IL-2, IL-7 and TNFα, are sensitive to low nanomolar concentrations of KZR-8445, while the SPs of other Sec61 substrates are insensitive with IC_{50} values > 25 μM.[12]

Besides HUN-7293, most natural Sec61 inhibitors have apparently evolved to inhibit ER translocation of a broad range of Sec61 substrates and are eventually cytotoxic.[2,12,18,29] This general mechanism underlies the pharmacological properties of several natural and synthetic Sec61 inhibitors against solid and hematological cancer cell types.[21,30−35] Human cancer cells are sensitive to low nanomolar concentrations of CbA (**1**), which can be attributed, at least initially, to the functional loss of a broad-range of Sec61 client proteins that are critical for cell proliferation and survival.[1,3,33,36−38] Consistent with other Sec61 inhibitors of ER protein import, **1** promotes the degradation of Sec61 clients displaced to the cytosolic compartment. In addition, **1** triggers cell death in concentration- and time-dependent manners when proteostasis is lost.[2,3,36,37,39] Unfortunately, this primary mechanism of action also underlies the potential of broad-spectrum Sec61 inhibitors to induce off-target toxicity.[2] Early evaluation of antitumor efficacy of **1** in mice bearing subcutaneous xenografts revealed an adverse safety profile after repeat dosing of the unmodified natural product.[33] Since then, extensive structure−activity relationship (SAR) studies have identified critical elements of the molecular substructure that render high cytotoxicity of **1** and show the feasibility of generating synthetically accessible analogues that retain antitumor activity without inducing subacute toxicity.[40,41] However, the most promising broad-spectrum Sec61 inhibitor developed to date is a synthetic small molecule termed KZR-261 that potently inhibits the expression of multiple Sec61 substrates including VEGF, VEGFR, and EGFR.[34] KZR-261 demonstrated antitumor efficacy and was well tolerated in multiple animal models of solid and hematological cancers, which resulted in a multi-center Phase 1 clinical trial in patients with advanced solid malignancies.[34]

Although all Sec61 inhibitors are predicted to bind and compete for a common region within the Sec61α subunit, extensive resistance mapping in cells and advanced structural models have confirmed that these ligands form nonidentical interactions with Sec61.[3,12,14,17,18,21,42] Point mutations in Sec61α conferring strong resistance to the broad-spectrum cyanobacterial Sec61 inhibitor apratoxin A (AprA), confer only mild resistance to **1**, which suggests that the two molecules bind distinct interfaces or possibly different conformational states of the native channel.[3] Moreover, it is unclear why some secretory and Type-I membrane proteins are more sensitive to CbA (**1**), or AprA, than closely related Sec61 clients with similar primary sequence homology.[37,43,44] Given the structural complexity and physiochemical properties of lariat depsipetide scaffolds,[45] the present study aimed to assess the potential impact of stereoselectivity on the action of **1**. Several research groups have previously shown that single alterations in the stereochemistry of chiral centers in the macrocycle, or tail, of **1**, results in significant decreases in cytotoxic potency relative to the authentic natural product.[1,36,40,46−48] We compared the pharmacological properties of **1**, and two major diastereoisomers, against a panel of patient-derived glioblastoma (GBM) stem-like cells (GSCs) with clinically relevant features of GBM including the amplification of known Sec61 substrates such as EGFR and PDGFR (Figure S1). GBM is the most malignant and common type of primary brain tumor, resulting in significant mortality due to a lack of effective therapeutic options.[49] Upregulation of the Sec61 gamma subunit was first described in GBM patient tumors, relative to low-grade glioma and normal astrocytes,[50,51] and has subsequently been reported in several other cancers with poor prognosis.[52−55] Diastereomers of **1** were selected based on their ability to inhibit the expression of a secreted *Gaussia* luciferase (GLuc) reporter with nanomolar potency and the relative resistance of cells harboring a single mutation in Sec61α versus decreased viability observed in wild-type (WT) cells. We evaluated the expression of representative proteins typically trafficked through Sec61-dependent and Sec61-independent pathways in response to treatment. Our results indicate that specific

https://doi.org/10.1021/acsptsci.4c00049
ACS Pharmacol. Transl. Sci. 2024, 7, 1823−1838

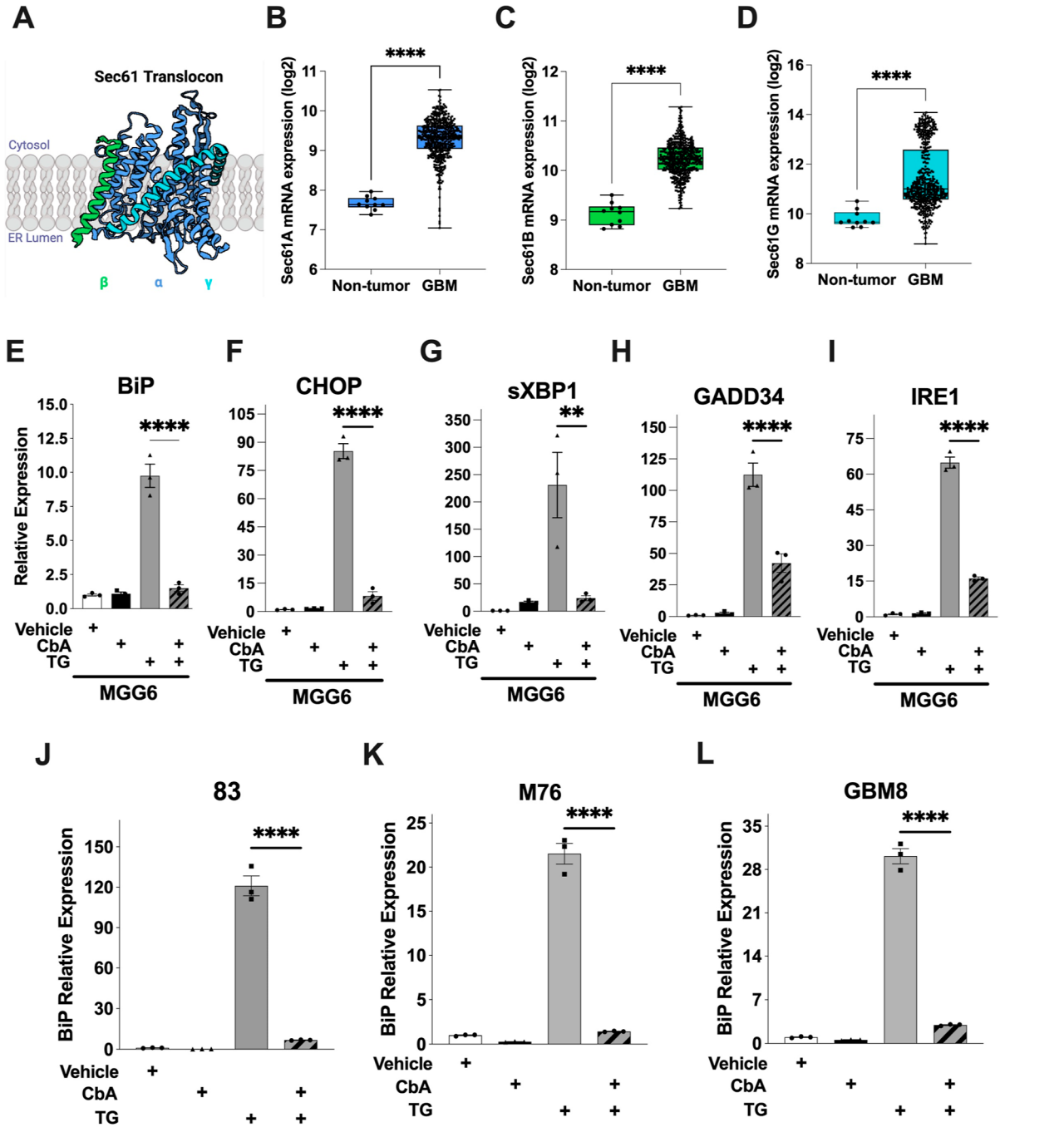

Figure 1. Coibamide A impairs UPR signaling in patient-derived glioma stem-like cells (GSCs). (A) Representation of the human Sec61 translocon channel complex in the ER membrane, adapted from.[18] (B–D) mRNA expression of Sec61A1, (B,G) subunits in nontumor versus primary GBM tissue (TCGA data set). (E–I) Relative mRNA expression of UPR markers (BiP, CHOP, sXBP1, GADD34, IRE1) in MGG6 GSCs treated with vehicle (0.1% DMSO), coibamide A (CbA; 80 nM), thapsigargin (TG; 300 nM), or cotreated with CbA and TG for 24 h determined by qPCR normalized to GAPDH. (J–S) Relative mRNA expression of BiP in 83, M76 and GBM8 GSCs treated as above and determined by qPCR. Data is expressed as fold-change compared to vehicle. Statistical significance of change is $^{**}p < 0.01$, $^{****}p < 0.001$.

changes in the stereochemical configuration of CbA can be tolerated to yield CbA-like molecules with distinct Sec61 substrate preferences and pharmacological signatures.

RESULTS AND DISCUSSION

Coibamide A Impairs ER Stress Signaling in Human Glioma Stem-like Cells. Analysis of the TCGA database has previously revealed a statistically significant upregulation of Sec61 subunits in primary GBM tumors relative to normal brain (Figure 1A–D), and highlighted a specific role for Sec61 gamma as a biomarker of GBM adaptation to ER stress and poor therapeutic response in GBM patients.[50,56] Given the high sensitivity of established GBM cell lines to CbA,[1,33,36] we studied the ability of CbA to modulate the unfolded protein response (UPR) in patient-derived GSCs for the first time. Cancer stem cells are a major driver of disease progression and recurrence in GBM. They can retain aggressive, stem cell properties in culture that more faithfully model key features of

https://doi.org/10.1021/acsptsci.4c00049
ACS Pharmacol. Transl. Sci. 2024, 7, 1823–1838

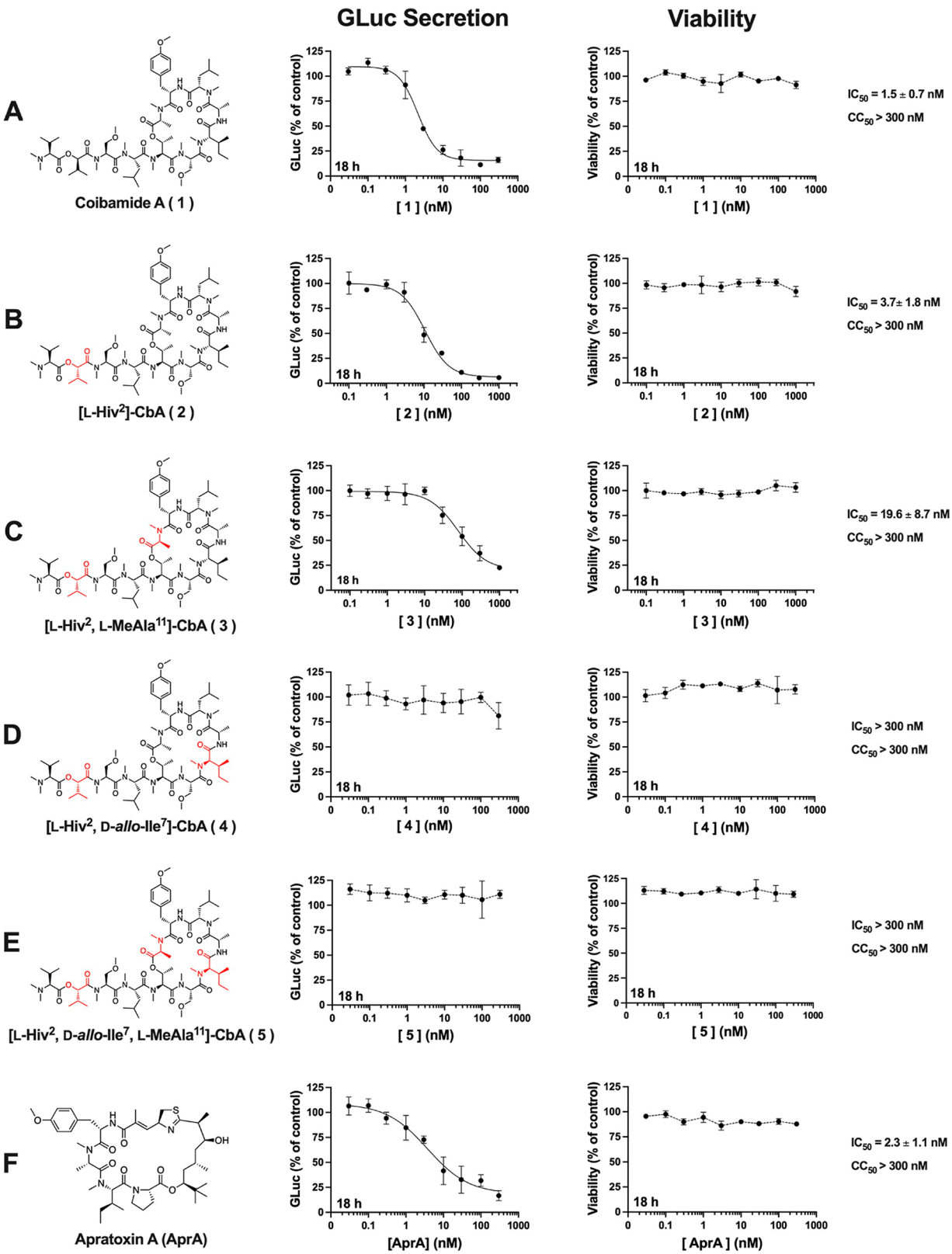

Figure 2. Stereochemical SAR for Inhibition of Secretory Function by Diastereoisomers of Coibamide A. Molecular structures and bioactivity profile of (A) coibamide A (1), (B) [L-Hiv^2]-CbA (2), (C) [L-Hiv^2, L-MeAla^{11}]-CbA (3), (D) [L-Hiv^2, D-allo-Ile^7]-CbA (4), (E) [L-Hiv^2, D-allo-Ile^7, L-MeAla^{11}]-CbA (5) and (F) apratoxin A (AprA). Secretory function of human U87-MG cells expressing *Gaussia* luciferase (GLuc) was assessed in the presence or absence (0.1% DMSO), of compounds. After 18 h, GLuc activity was measured in conditioned medium while viability was assessed in the adherent Gluc-U87 cells. Data points show mean luminescence ± standard error (S.E.) as a percentage of vehicle-treated cells and curves represent the fit of data points by nonlinear regression analysis to a logistic equation from a comparison that was repeated in at least three independent experiments.

https://doi.org/10.1021/acsptsci.4c00049
ACS Pharmacol. Transl. Sci. 2024, 7, 1823−1838

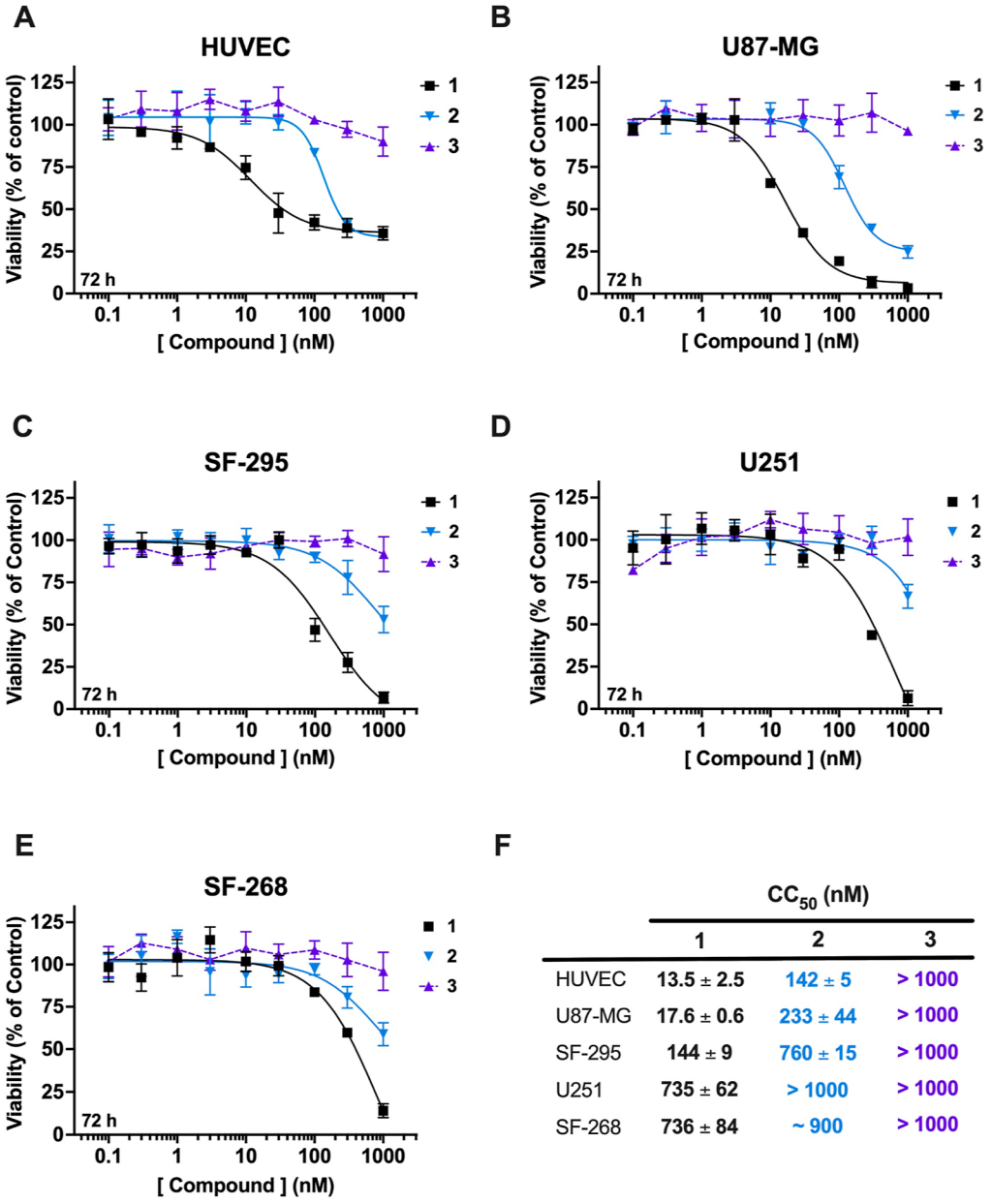

Figure 3. Relative toxicity of coibamide A, [L-Hiv^2]-CbA, and [L-Hiv^2,L-MeAla^{11}]-CbA to normal endothelial cells and established GBM cells. Viability of (A) human umbilical cord vein cells (HUVECs) and human (B) U87-MG, (C) SF-295, (D) U251, and (E) SF-268 GBM cells in response to treatment for 72 h long treatment with increasing concentrations of 1−3 or vehicle (0.1% DMSO). Cell viability was calculated as a percentage of response to vehicle. Graphs represent mean viability ± S.E. (n = 3 wells per treatment) and curves represent the fit of data points by nonlinear regression analysis to a logistic equation. (F) Values represent cytotoxic concentrations for 50% inhibition (CC_{50} ± S.E.) relative to control, from three independent comparisons.

GBM, such as cellular heterogeneity and treatment resistance, than established GBM cell lines.[57,58] In preliminary studies, exposure of GSC 157 neurospheres to **1** (100 nM), or AprA (100 nM), induced similar changes in cell morphology characterized by a reduction in neurosphere size at 24 h relative to control-treated cells (Figure S2A). Expression of ER stress marker transcripts was then measured in several GSC lines after treatment with CbA (80 nM), thapsigargin (300 nM), or CbA plus thapsigargin relative to vehicle (0.1% DMSO)-treated neurospheres. As anticipated, pharmacological induction of ER stress with thapsigargin induced marked upregulation of BiP, CHOP, sXBP1, GADD34, and IRE1 mRNA expression in GSCs (Figure 1E−L). However, treatment with CbA almost completely abrogated thapsigargin-induced upregulation of all UPR markers in GSC line MGG6 (Figure 1E−I), and BiP mRNA expression in three additional GCS cell lines (Figure 1J−L). BiP was previously validated as a coibamide-sensitive Sec61 substrate in cell-free translocation assays,[3] and thus we also analyzed BiP protein expression in response to **1**. Immunoblot analysis revealed downregulation of BiP expression in GSC MGG6 neurospheres and adherent U87-MG cells (Figure S2B,C) consistent with coibamide-induced block of BiP import into the ER by **1**[3] and degradation by the ubiquitin-proteosome system (Figure S2C). Under normal conditions, BiP binds to and blocks the activation of all three branches of the UPR.[59] The dissociation

https://doi.org/10.1021/acsptsci.4c00049
ACS Pharmacol. Transl. Sci. 2024, 7, 1823−1838

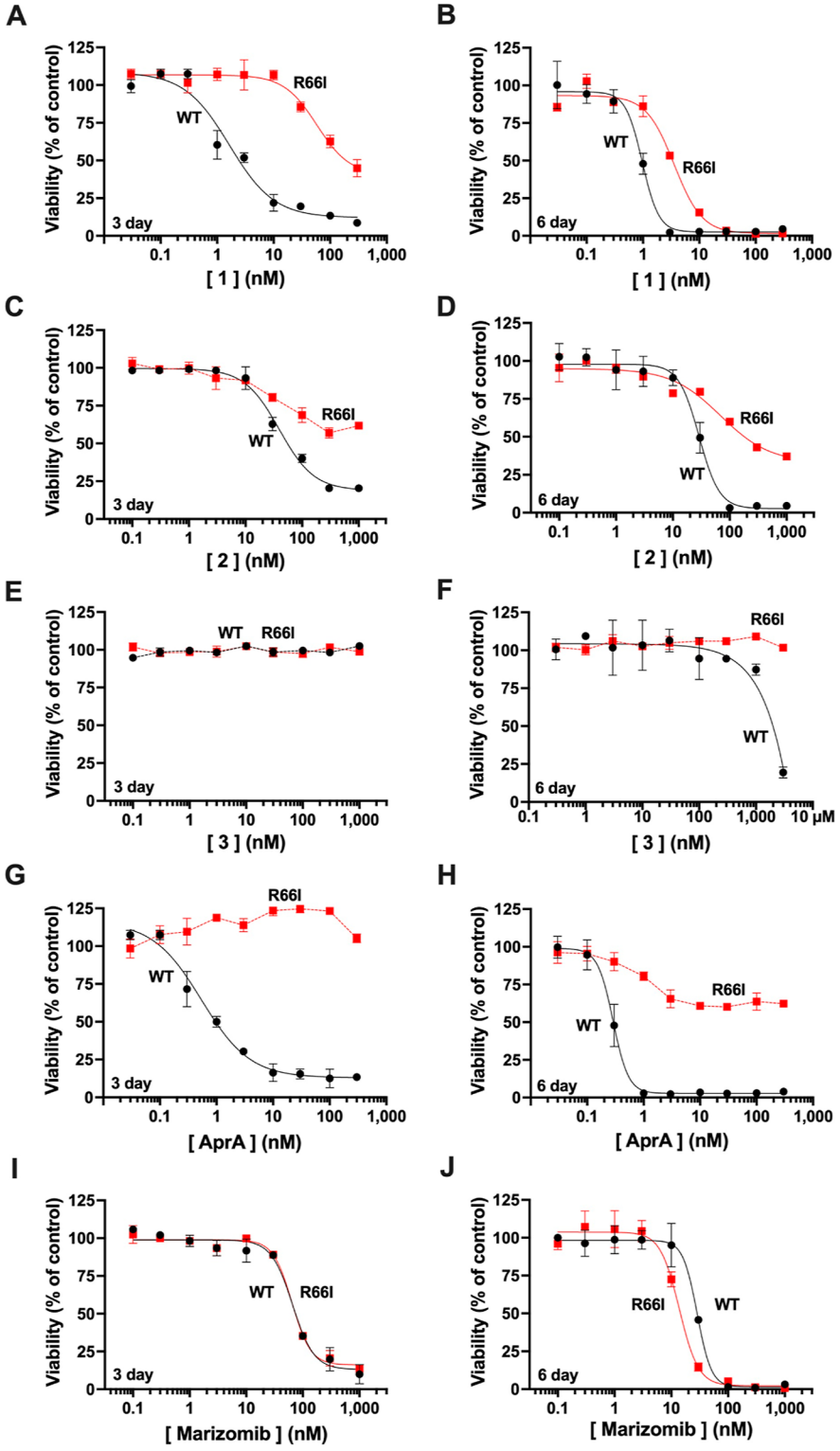

Figure 4. Sec61α confers sensitivity to [L-Hiv^2]-CbA and [L-Hiv^2,L-MeAla^{11}]-CbA. Concentration- and time-dependent responses in human WT and mutant (R66I) Sec61α HCT116 colon cancer cells to the treatment with (A,B) coibamide A (1), (C,D) [L-Hiv^2]-CbA (2), (E,F) [L-Hiv^2, L-MeAla^{11}]-CbA (3), (G,H) apratoxin A (AprA), or (I,J) marizomib. Cell viability was assessed 72 h or (3 + 3 days) after the exposure to compound or vehicle (0.1% DMSO). Data points show mean viability ± S.E. (n = 3 wells per treatment) as a percentage, relative to vehicle-treated cells and curves represent the fit of data points by nonlinear regression analysis to a logistic equation from a comparison repeated in at least three independent experiments.

of BiP from these proteins,[60] or its downregulation,[61,62] activates UPR signaling. Although **1** inhibits biosynthesis of a broad range of Sec61 substrates,[3] these results suggest that GSCs may be particularly vulnerable to a loss of Sec61 function and the ability to maintain proteostasis in response to ER stress.

https://doi.org/10.1021/acsptsci.4c00049
ACS Pharmacol. Transl. Sci. 2024, 7, 1823−1838

Select Diastereomers of Coibamide A Retain Functional Activity in Living Cells. A stereochemical SAR for evaluating the potent nanomolar toxicity of CbA (**1**) was first appreciated during independent approaches to total synthesis of the originally proposed structure.[1,46−48] Both [L-Hiv^2]-coibamide (**2**, where Hiv is 2-hydroxyisovaleric acid), developed by us, and the "all-L" [L-Hiv^2, L-MeAla^{11}]-coibamide (**3**), developed by Yao and co-workers, showed a significant decrease in cytotoxic potency against all cancer cell lines tested using standard end-point cell viability assays.[46,47] Fang, Su and co-workers subsequently reported a stereochemical revision at two of the 13 chiral centers, as D-Hiv^2 in the side chain and D-MeAla^{11} in the macrocycle, that was confirmed to match the configuration and cytotoxic potency of natural **1** (Figure 2A).[48,63] To determine if changes in stereochemistry impact the ability of **1** to inhibit secretory function in living cells, we utilized a whole cell assay, in which human U87-MG glioblastoma cells stably expressing GLuc were treated with four synthetic diastereoisomers of **1**. GLuc is a nontoxic, naturally secreted, photoprotein with a classic N-terminal SP and thus served as a convenient model Sec61 client protein for reporting on the secretory function of living cells in culture.[64] Maintaining an L configuration of 2-hydroxyisovaleric (Hiv) acid at position 2 in the peptide chain, the configurations of Ile at position 7 and MeAla at position 11 were systematically inverted. GLuc-U87 cells were treated with increasing concentrations of **1** (CbA), **2** ([L-Hiv^2]-CbA), **3** ([L-Hiv^2, L-MeAla^{11}]-CbA), **4** ([L-Hiv^2, D-*allo*-Ile^7]-CbA), **5** ([L-Hiv^2, D-*allo*-Ile^7, L-MeAla^{11}]-CbA), AprA, or vehicle (0.1% DMSO). After 18 h, aliquots of conditioned medium were measured for bioluminescence in the presence of the GLuc substrate coelenterazine, and all adherent cells were assessed at the same time for viability by quantification of ATP. As anticipated from previous testing,[37] **1** and AprA (0.3−300 nM) induced concentration-dependent decreases in GLuc expression in the cell culture medium with no change in cell viability at 18 h (Figure 2A,F). Diastereoisomers **2** (0.1 nM−1 μM) and **3** (0.1 nM−1 μM) also produced concentration-dependent decreases in GLuc expression in viable cells, indicating that inversion of the Hiv^2 configuration in the CbA side chain alone (Figure 2B), or in combination with inversion of MeAla^{11} in the macrocycle (Figure 2C), was not sufficient to destroy functional inhibition of GLuc secretion by these two molecules. In contrast, substitution of L-Ile^7 in the macrocycle with D-*allo*-Ile, either alone (**4**; Figure 2D) or in combination with inversion of MeAla^{11} (**5**; Figure 2E) resulted in a loss of functional efficacy relative to **1**−**3** or AprA. These findings are consistent with the conclusion that **1** has a well-defined conformation that is highly sensitive to any changes in stereochemistry of the chiral centers in the macrocycle or side chain.[40] As **2** and **3** retained the ability to inhibit GLuc secretion with nM potency, we focused the rest of our study on these two functionally active diastereomers of **1**.

[L-Hiv^2]-CbA and [L-Hiv^2, L-MeAla^{11}]-CbA Target Sec61 and are Less Toxic than Coibamide A. The relative cytotoxicity of **2** and **3** was compared in normal human umbilical endothelial vein cells (HUVECs) and four established human glioblastoma cell types (U87-MG, SF-295, U251, and SF-268). All cells were exposed to increasing concentrations of **1** (0.1 nM−1 μM), **2** (0.1 nM−1 μM), **3** (0.1 nM−1 μM), or vehicle (0.1% DMSO) for 72 h and assessed for viability by quantification of ATP relative to control cultures (Figure 3A−E). In all comparisons, **2** and **3** were less cytotoxic than **1** with **3** showing the greatest loss of cytotoxic potency and efficacy under these assay conditions (Figure 3F). These findings served to confirm and extend the results of individual testing of **2** or **3** alone, where a change in the configuration at position 2 was associated with a 4- to 8-fold decrease in cytotoxic potency relative to **1**[47] and the cytotoxic efficacy of **3** was shifted to the micromolar range.[46] Consistent with the results of earlier comparative testing of **2** against a mixed panel of established cancer cell types representing human lung, breast, prostate, and GBM,[47] the magnitude of the change in sensitivity to **2** varied across GBM cell types tested and was not necessarily predicted (Figure 3B−F). For example, U87-MG cells were most sensitive to **1** and **2**, with **2** being approximately 13-fold less potent than **1**. However, **2** was only 5-fold less sensitive than **1** against SF-295 cells (Figure 3F). In contrast, U251 and SF-268 cells were inherently less sensitive to **1** (EC_{50} > 700 nM) than U87-MG cells (EC_{50} = 18 nM) and thus the magnitude of change in sensitivity to **2** was less (Figure 3F). These results continue to support the observation that human cancer cells show differential sensitivity to individual Sec61 inhibitors and that structural refinement of the CbA pharmacophore may ultimately yield target-specific ligands that retain anticancer efficacy with a more favorable safety profile.

To determine if **2** and **3** retain the ability to interact with the Sec61 translocon channel, we utilized HCT116 colon cancer cells harboring a single point mutation (R66I) in the plug region of the Sec61α subunit. This R66I mutation was previously identified in a chemogenetic screen and conferred mild resistance to **1** and strong resistance to several other substrate-selective and broad-spectrum Sec61 inhibitors.[2,3,21] WT and R66I mutant HCT116 colon cancer cells (Figure 4), or HEK293 cells engineered with the same mutation (Figure S3), were exposed to increasing concentrations of **1** (0.03 nM−300 nM), **2** (0.3 nM−1 μM), **3** (0.3 nM−3 μM), AprA (0.03 nM−300 nM) or an unrelated proteasome inhibitor, marizomib (0.03 nM−1 μM), for either 72 h or 6 days (using a 3 + 3 day exposure to avoid nutrient deprivation[65]). As anticipated, side-by-side cell viability testing revealed a shift in the concentration−response relationship of the R66I cells to **1**, reflecting mild resistance (Figure 4A;[3]), that was maintained after extended exposures (Figure 4B). Concentration−response analysis of **2** also revealed a decrease in cytotoxic efficacy in Sec61 (R66I) cells at both assay end points relative to WT HCT116 cells (Figure 4C,D). In contrast, **3** induced no change in the cell viability at 72 h (Figure 4E), and a pattern of resistance was revealed in the R66I mutant cells at the extended end point (Figure 4E,F). The R66I mutation conferred strong resistance to AprA (Figure 4G,H) and did not change the cytotoxic efficacy of marizomib (Figure 4I,J). These patterns of resistance to **2** and **3** were maintained in HEK293 cells engineered to stably express the same Sec61-(R66I) mutation relative to WT cells (Figure S3). Further, mutant Sec61(R66I) HEK293 cells were resistant to **1** and AprA yet remained highly sensitive to marizomib (Figure S3A−J). These data strongly suggest that diastereomers **2** and **3** retain structural conformations that are sufficient for target engagement with Sec61 and that R66I, located in the mobile plug region of the Sec61α subunit,[18] is either in contact with, or modulated by, **2** and **3**.

[L-Hiv^2]-CbA and [L-Hiv^2, L-MeAla^{11}]-CbA Inhibit Expression of Secreted and Transmembrane Sec61 Clients. To explore the selectivity profile of **2** and **3**, beyond

https://doi.org/10.1021/acsptsci.4c00049
ACS Pharmacol. Transl. Sci. 2024, 7, 1823−1838

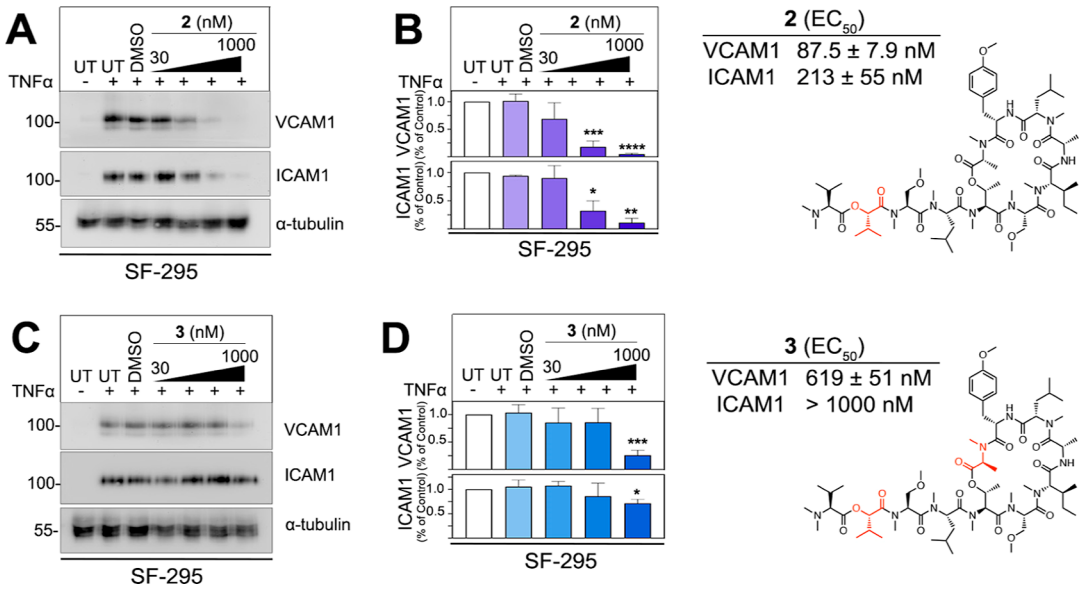

Figure 5. Cytokine-induced expression of endogenous VCAM1 and ICAM1 is suppressed by [L-Hiv^2]-CbA and [L-Hiv^2,L-MeAla^{11}]-CbA. Immunoblot analysis of type 1 cell adhesion molecules VCAM1 and ICAM1 in human SF-295 glioblastoma cells exposed to increasing concentrations of [L-Hiv^2]-CbA (**2**) or [L-Hiv^2, L-MeAla^{11}]-CbA (**3**), relative to vehicle (0.1% DMSO)-treated and untreated (UT) cells for 24 h. SF-295 cells were cotreated with **2** or **3** in the presence of TNFα (10 ng/mL). Images in panels (A,C) show representative expression of cell adhesion molecules relative to loading control (αtubulin). Quantifications of immunoblot data from three independent experiments are shown on panels (B,D). Statistical significance of change relative to vehicle (0.1% DMSO) is *$p < 0.05$, **$p < 0.01$, ***$p < 0.005$, ****$p < 0.001$.

potent inhibition of GLuc secretion (Figure 2), we compared the impacts of these diastereomers on the expression of several proteins that are typically trafficked through Sec61-dependent or Sec61-independent pathways. We surveyed the relative expression of two surface adhesion Sec61 clients, VCAM1 and ICAM1, previously used to define the SAR of the cotransins.[23,25] For these studies, human SF-295 cells were pretreated with the proinflammatory cytokine TNFα (10 ng/mL) to stimulate the expression of endogenous VCAM1 and ICAM1. Immunoblot analysis of cell lysates with or without increasing concentrations of **2**, **3**, or vehicle (0.1% DMSO) showed concentration-dependent decreases in VCAM1 and ICAM1 expression after 24 h. Both cell adhesion proteins were significantly downregulated in response to **2** (Figure 5A,B) and **3** (Figure 5C,D). VCAM1 was approximately 7-fold more sensitive to **2** (IC_{50} = 88 nM) than **3** (IC_{50} = 620 nM) and VCAM1 was more sensitive than ICAM1 to both compounds (Figure 5). Although less potent than **1** (Figure S4A,B;[3]), **2** was fully efficacious, and **3** was partially effective in suppressing TNFα-stimulated VCAM1 expression in SF-295 cells (Figure S4A,B). Diastereomers **2** and **3** also induced statistically significant decreases in the level of VCAM1 transiently expressed in HEK293 cells (Figure S4C,D).

In a comparison of the expression of BiP, a second secreted ER-resident protein [calreticulin (CALR)], three cytosolic heat shock proteins (Hsp90, Hsp70, and Hsp40), and two multipass transmembrane proteins [Sec61α and multidrug resistance 1 (MDR1)], only BiP (Figure 6A−D) and CALR (Figure 6A,B) were downregulated in response to the treatment. In the presence of a relatively high (1 μM) concentration of each diastereomer, fixed at 50-fold higher than the IC_{50} for GLuc inhibition by **3**, BiP was suppressed by **2** in normal HUVECs and U87-MG GBM cells, whereas **3** induced no statistically significant change in BiP (Figure 6A,B). CALR showed a similar expression pattern in response to **1**−**2** and was less sensitive to **3** (Figure 6A,B). In contrast, **1**−**3** induced a statistically significant upregulation of Hsp40 in U87-MG cells, while **1** and **2** also induced upregulation of Hsp70 and Hsp90 (Figure 6A,B). None of the compounds (**1**−**3**) induced statistically significant changes in the expression of Sec61α or MDR1 (Figure 6A,B), consistent with previous studies concluding that multipass transmembrane proteins undergo Sec61-independent biogenesis at the ER membrane.[3,20,66,67] Compensatory upregulation of cytosolic Hsps has been noted in response to Sec61 inhibition,[68] and thus these observations suggested that the bioactivity profile of **2** and **3** was similar to **1**.

Given that relatively high concentrations are required to inhibit the expression of VCAM1, ICAM1, BiP, or CALR, relative to the potency with which **2** and **3** inhibited GLuc (IC_{50} < 20 nM), we extended our survey of extracellular proteins. A pattern, whereby Sec61-dependent secreted proteins are more sensitive than membrane proteins, has been previously noted for cotransin,[28] and thus, we submitted conditioned medium from SF-268 glioblastoma cell cultures for independent quantification against a panel of human cytokines and chemokines (Figure 7). In preliminary studies, **2** and **3** induced statistically significant inhibition of VEGF-A (a CbA-sensitive Sec61 client[33]) at 24 h (Figure S5A) and this inhibition was sustained 24 h after removal of **2** and **3** and replacement with serum-free medium (Figure S5B,C). Toward the goal of defining the most sensitive population of proteins, conditioned medium was, therefore, collected 24 h after removal of **2** (1 μM), **3** (1 μM), or vehicle (0.1% DMSO) and submitted for analysis (Figure 7). Of the 43 different secreted proteins quantified in the SF-268 secretome, the expression of 24 proteins was decreased by <50% after exposure to **2** (Figure 7A), and the expression of 18 proteins was decreased by <50% after **3** (Figure 7B), relative to protein expression in vehicle-treated cells. Sensitive proteins were generally predicted to be trafficked via Sec61 (Table S1); however, the rank order of sensitivity of proteins to **2** was different from that of **3** (Figure

https://doi.org/10.1021/acsptsci.4c00049
ACS Pharmacol. Transl. Sci. 2024, 7, 1823−1838

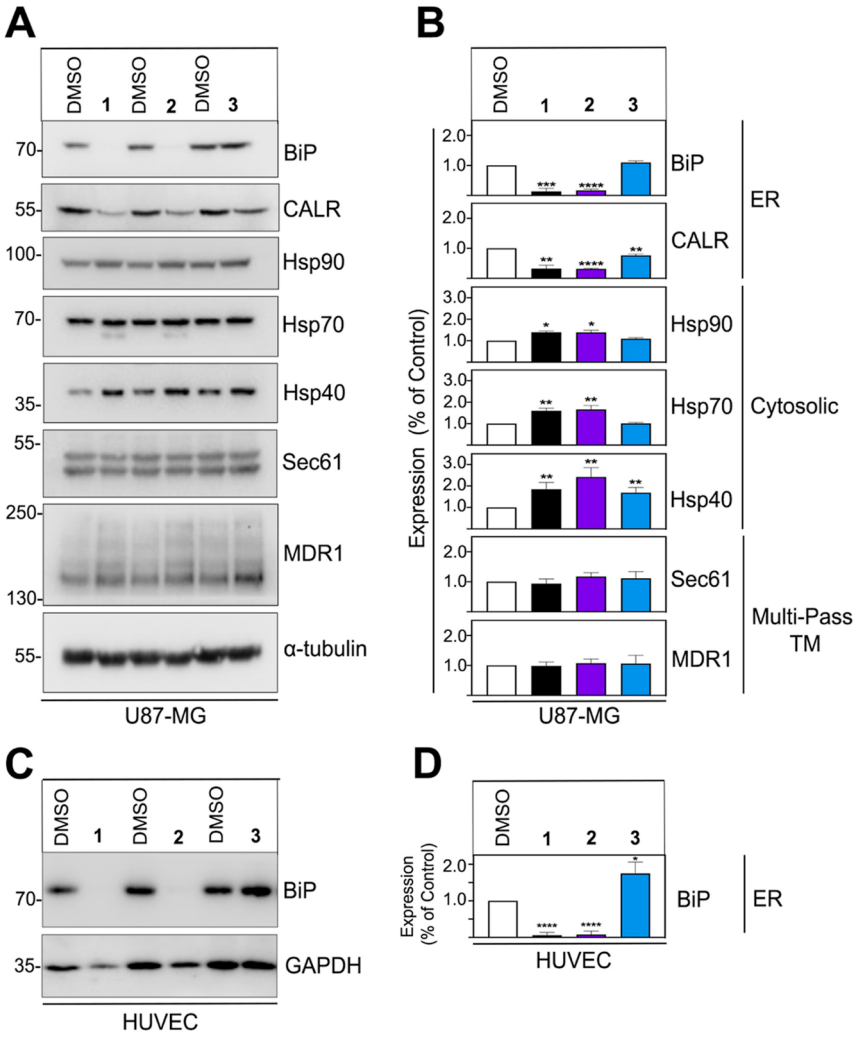

Figure 6. Expression analysis of representative Sec61 and non-Sec61 client proteins in response to [L-Hiv^2]-CbA and [L-Hiv^2,L-MeAla^{11}]-CbA. (A) Expression of ER secretory pathway [BiP, calreticulin (CALR)], cytosolic heat shock (Hsp90, Hsp70, Hsp40), and polytopic transmembrane (Sec61α subunit, MDR1) proteins relative to α-tubulin (loading control) in human U87-MG glioblastoma cells exposed to 1 (30 nM), [L-Hiv^2]-CbA 2 (1 μM), [L-Hiv^2, L-MeAla^{11}]-CbA 3 (1 μM), or vehicle (0.1% DMSO) for 24 h. (B) Quantification of immunoblot data (panel A) from three independent experiments. (C) Immunoblot analysis of BiP and GAPDH (loading control) in HUVECs in response to 1 (30 nM), [L-Hiv^2]-CbA 2 (1 μM), [L-Hiv^2, L-MeAla^{11}]-CbA 3 (1 μM), or vehicle (0.1% DMSO) for 24 h. (D) Quantification of immunoblot data (panel C) from three independent experiments. Statistical significance of change relative to vehicle (0.1% DMSO) is $^*p < 0.05$, $^{**}p < 0.01$, $^{***}p < 0.005$, $^{****}p < 0.001$.

7A−C). For example, IL-15, VEGF-A, and IFN-*gamma* represented the top three most sensitive proteins to **2** (Figure 7A), whereas these three proteins were not the top three proteins most sensitive to **3**; VEGF-A was the second most sensitive protein to **2** (IC_{50} = 13 nM) and the twelfth most sensitive protein to **3** (IC_{50} = 171 nM) (Figures 7B and S5C). These results expand the range of known Sec61 substrates inhibited by CbA compounds to include other growth factors, interleukins, and chemokines. Further, the striking differential sensitivity of secreted proteins to **2** and **3** (Figure 7C) suggested that these diastereomers have distinct pharmacological signatures, presumably due to subtle differences in the spatial arrangement of **1**, **2**, and **3** within the Sec61 inhibitor-binding pocket.[3,18]

Human Glioma Stem-like Cells are Differentially Sensitive to Coibamide A, [L-Hiv^2]-CbA, and [L-Hiv^2, L-MeAla^{11}]-CbA. Six different GSCs isolated from patients with primary or recurrent GBM, collectively representing a range of distinct molecular features with clinical significance (Figure S1), were used to compare the bioactivity profiles of **2** and **3**. For these studies, all GSCs were expanded and maintained in suspension as neurospheres before exposure to increasing concentrations of **1**, **2**, and **3**, or vehicle (0.1% DMSO) for 72 h. The viability of 5/6 GSC lines tested was dramatically reduced by exposure to sub- to low nanomolar concentrations of **1** (EC_{50} < 4 nM), with only GSC type 83 showing reduced sensitivity to **1** (EC_{50} ∼ 100 nM), and relative resistance to **2** and **3** (Figure 8A−C). The same five GSC lines (M120, MGG6, M76, GBM8, and 157) were also sensitive to sub- to low micromolar concentrations of **2** or **3** (Figure 8D−G), with EC_{50} values of <3 μM for **2** (Figure 8E) and <6 μM for **3** (Figure 8G). GSC line 83 was also the least sensitive to **2** or **3** (up to 16 μM) in these assays (Figure 8D−G). Remarkably, the five coibamide-sensitive GSCs showed differences in the rank order of sensitivity to **1**, **2**, and **3**, suggesting that stereochemical rearrangement of **1** generates bioactive diastereomers that behave as distinct compounds and confer some degree of GSC type-specific toxicity through broad

https://doi.org/10.1021/acsptsci.4c00049
ACS Pharmacol. Transl. Sci. 2024, 7, 1823−1838

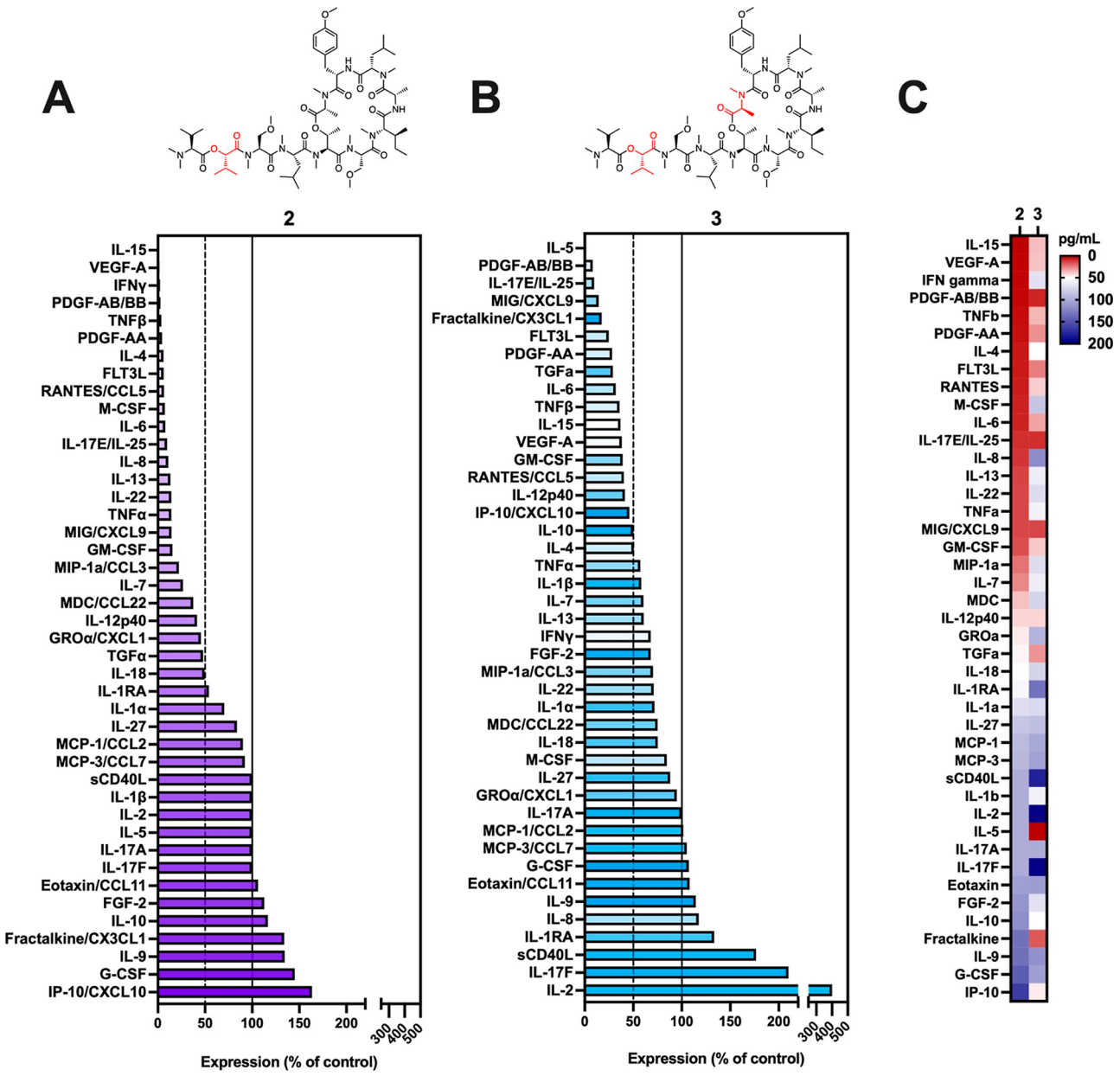

Figure 7. Differential inhibition of secreted human cytokines/chemokines by [L-Hiv^2]-CbA and [L-Hiv^2,L-MeAla^{11}]-CbA. Secretome analysis of cytokine/chemokine released into the medium of human SF-268 glioblastoma cells 24 h after removal of (A) [L-Hiv^2]-CbA 2 (1 μM), or (B) [L-Hiv^2, L-MeAla^{11}]-CbA 3 (1 μM). After 24 h incubation, cell culture medium containing test compound or vehicle (0.1% DMSO) was removed and replaced with serum-free medium for an additional 24 h. Expression of proteins in the conditioned-medium was analyzed by addressable multiplex laser-bead immunoassay (by Eve Technologies Corp.) and expressed as a percentage expression in vehicle-treated cells. (C) The resistance (blue) and sensitivity (red) of secreted proteins detected in the conditioned medium (pg/mL) ranked as a heatmap.

inhibition of ER protein import. This kind of selective vulnerability of human cancer cells to individual Sec61 inhibitors has been noted following comparative analysis of cytotoxicity to **1**, AprA, and the plant-derived Sec61 inhibitor ipomoeassin F.[2,3] Although all three structures target Sec61, phenotypic screening against the same National Cancer Institute 60 (NCI-60) human tumor cell line panel resulted in distinct selectivity profiles for each ligand.[2,3] These data expand this observation to reveal differences in the sensitivity of GSCs to specific stereoisomers of **1**.

The extreme heterogeneity of GBM and the discovery of subpopulations of GSCs within the same tumor mass that exhibit phenotypic, functional, and metabolic plasticity continues to represent a significant barrier to the successful development of new single-agent therapeutics.[69−72] Thus, the cytotoxic potency and efficacy of **1**−**3** were surprising in that most of the GSCs within the small panel used in the present study were affected. As a group, the CbA-sensitive GSCs represented proneural (M120, MGG6, 157, GBM8), classical (M76) and mesenchymal-like (83) subtypes each with a range of different genetic alterations (Figure S1). The gene encoding the *gamma* subunit of Sec61 is located with *EGFR* on the region of human chromosome 7p11.2 that is frequently amplified in GBM leading to overexpression of Sec61 gamma in primary GBM with EGFR amplification.[50,56,69,73] However, **1**−**3** were not more selective for GSCs with EGFR amplification, suggesting that the loss of other Sec61 client proteins may be as critical to GSC viability as the maintenance

https://doi.org/10.1021/acsptsci.4c00049
ACS Pharmacol. Transl. Sci. 2024, 7, 1823−1838

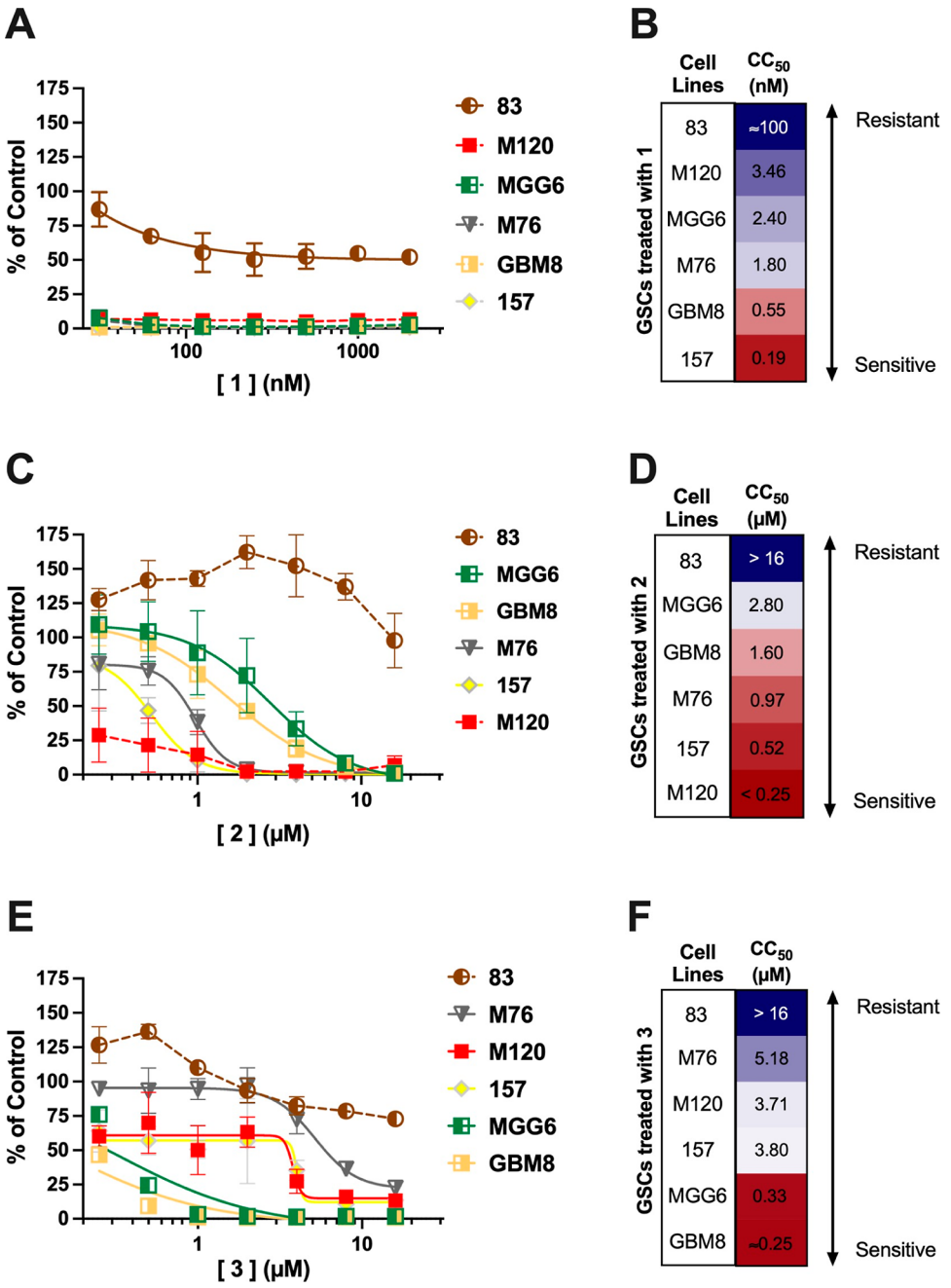

Figure 8. Patient-derived glioma stem cells (GSCs) are differentially sensitive to coibamide A, [L-Hiv^2]-CbA, and [L-Hiv^2,L-MeAla^{11}]-CbA. Viability of six different patient-derived GSCs exposed to increasing concentrations of (A,B) CbA 1, (C,D) [L-Hiv^2]-CbA 2, (E,F) [L-Hiv^2, L-MeAla^{11}]-CbA 3, or vehicle control (0.1% DMSO) for 72 h. The resistance (blue) and sensitivity (red) of the cells to the compounds at the mean cytotoxic concentration that reduces the cell viability by 50% (CC_{50}) was ranked for each compound as a heatmap: (B) 1, (D) 2, and (F) 3.

of intracellular ER protostasis. For example, the ability of these ligands to broadly suppress autocrine signaling at low nanomolar concentrations, and disrupt the biosynthesis of tumor-supportive chemotactic signals, may represent a particularly desirable pharmacologic property. CbA and AprA are also potent inhibitors of protein glycosylation and maturation in the ER, resulting in the polyubiquitination and proteasomal degradation of immature forms of Sec61-dependent client proteins[3,33,37,74] (Figure S2C). In this context, the tumor-supporting function of the Sec61 channel complex, and the potential for targeting Sec61 in GBM to enhance CD8+ T-cell mediated cytotoxicity has been recently demonstrated by Zeng and coauthors.[73] The glycosylation status of immune checkpoint ligands, such as protein death-ligand 1 (PD-L1), is a critical determinant of PD-L protein stability and immune escape signaling.[75,76] Knockdown of *SEC61G*, or pharmacological inhibition of Sec61 with eeyarestatin, decreased glycosylation and increased the ubiquitination of several immune checkpoint ligands, while also increasing the infiltration and cytotoxic activity of CD8+ T-cells in immunocompetent mouse models of GBM.[73]

At present, the mechanistic basis for the reduced sensitivity of GSC line 83 to **1**−**3** is unclear. Immunoblot analysis of lysates prepared from GSC line 83 revealed a decrease in BiP expression in response to **1** and **2** (Figure S5D), providing indirect evidence of Sec61 target engagement in GSC line 83

https://doi.org/10.1021/acsptsci.4c00049
ACS Pharmacol. Transl. Sci. 2024, 7, 1823−1838

as observed in U87-MG cells and HUVECs (Figure 6A,C). Yet, these cells were least affected by all three ligands. Although the EGFR variant III (EGFRvIII) receptor (a feature of GSC line 83) maintains an N-terminal SP and is predicted to remain constitutively active at the cell membrane due to deficits in endocytosis,[77,78] further studies will be required to determine the extent to which nascent EGFRvIII relies on Sec61-dependent trafficking. In summary, this work highlights the potential utility of broad-spectrum Sec61 inhibitors as chemical probes to study how the loss of autocrine signaling and ER proteostasis induces cell death in GSCs. These studies also provide a framework for future optimization of Sec61 ligands to selectively inhibit the biosynthesis and maturation of tumor-supporting drivers of GBM that rely on the import of Sec61 into the ER secretory pathway.

MATERIALS AND METHODS

Chemicals, Reagents, and Plasmids. The isolation and purification of apratoxin A has been described previously.[79] Peptides **1**−**5** were synthesized by the identical procedure described previously with minor modifications.[3] Each compound was reconstituted in 100% cell culture grade DMSO Millipore-Sigma (Burlington, MA), aliquoted, and stored as concentrated (mM) stock solutions in amber borosilicate glass vials at −20 °C for use in biological studies. Marizomib and doxycycline were from MilliporeSigma (Burlington, MA), reconstituted in 100% DMSO, and stored at −20 °C. Coelenterazine was from Promega Corporation (Madison, WI) and was reconstituted in methanol. Recombinant human TNFα was purchased from Thermo Fisher Scientific Inc. (Carlsbad, CA) and was reconstituted in 5% bovine serum albumin in phosphate-buffered saline. Plasmids encoding *Gaussia* luciferase (GLuc) in a self-inactivating lentivirus vector for lentiviral transduction, and full length VCAM1 in the mammalian expression vector pCDNA3.1 for transient transfection studies was described previously.[3,37] All general laboratory reagents were from VWR International (Radnor, PA) and for titrations, compounds, or vehicle (0.1% DMSO) were delivered using a Hewlett-Packard (HP) D300 Digital Dispenser with HP Dispensing Software (version 3.2.2).

Primary Cells and Established Cell Lines. Human umbilical vascular endothelial cells (HUVECs), pooled from multiple donors (no. C01510C), were purchased from Thermo Fisher Scientific Inc. Primary GBM cells used in this study were dissociated from deidentified patient tumors and expanded as previously described.[80] MGG6 and GBM8 were provided by Dr. H. Wakimoto at MGH, M76 and M120 were provided by Dr. Sarkaria[69] at The Brain Tumor PDX National Resource at Mayo Clinic, and 157 and 83 were provided by Dr. Nakano.[70] In brief, GSCs were maintained in DMEM/F12 (Dulbecco's Modified Eagle Medium/Nutrient Mixture F-12) medium supplemented with B27 (without vitamin A; 1:50; Life Technologies), heparin (2 μg/mL; Sigma-Aldrich), human recombinant Epidermal Growth Factor (EGF; 20 ng/mL; ABM), and human recombinant basic fibroblast growth factor (bFGF-2; 10 ng/mL; ABM).

Human U87-MG and HEK-293T embryonic kidney cells were from the American Type Culture Collection (ATCC, Manasses, VA). U87-MG cells were infected with lentivirus in the presence of 8 μg/mL Polybrene (Sigma-Aldrich) as described previously,[37] to yield GLuc-U87 cells. Human SF-295, SF-268, and U251 glioblastoma cells were obtained from the National Cancer Institute (NCI) cell line repository (Fredrick, MD). Human HCT116 colon cancer cells with WT Sec61α and mutant R66I Sec61α, and HEK293FRT with the same Sec61α mutation, were generated at the University of Helsinki, Finland.[17] GLuc-U87, U87-MG, and U251 cells were cultured in Minimum Essential Medium (MEM) with Earl's salts and L-glutamine (Corning Life Sciences), supplemented with 10% fetal bovine serum (FBS; Hyclone, Logan, UT) and 100 U/mL penicillin and 100 mg/mL streptomycin (1% penicillin/streptomycinSF-268), HEK293T, and HEK293FRT cells were cultured in Dulbecco's Modified Eagle's Medium (DMEM) with 10% FBS, 1% penicillin/streptomycin, L-glutamine (6 mM), and sodium pyruvate (1 mM). SF-295 cells were cultured in RPMI 1640 medium with 10% FBS and 1% penicillin/streptomycin. HCT116 cells were cultured in McCoy's 5A medium supplemented with 10% FBS and 1% penicillin/streptomycin. All cells were grown under standard conditions and maintained at 37 °C in an atmosphere of 5% CO_2.

Quantitative Real-Time PCR (qPCR). All procedures for RNA extraction from GSCs and performing qPCR, the primer sequences for amplification of specific genes, and methods for quantification of relative mRNA expression have been described previously.[80]

***Gaussia* Luciferase (GLuc) Secretory Assay.** GLuc-U87 cells were seeded at 3000 cells/well into 96-well plates and allowed to adhere overnight. The next day, seeding medium was replaced with complete medium containing test compounds or vehicle, and plates were returned to the incubator. Following an 18 h treatment, 20 μL of the conditioned cell culture medium was removed from each well and transferred to 96-well white-walled plates. Subsequently, 50 μL of 1.68 μM coelenterazine was injected into each well for a final concentration of 1.2 μM, and luminescent signals were measured using a multimode microplate reader (Biotek Synergy HT) with Gen5 software and compared across conditions (3 s wait, 0.5 s integration time following coelenterazine injection).

Cell Viability Assays. Cell viability was assessed at the end point of each assay using a CellTiter-Glo Luminescent assay designed to detect ATP (Promega Corp.).

Analysis of Protein Expression by Western Blot and ELISA. For immunoblot analysis, cells were processed as described previously.[36] Lysates were adjusted for protein content using a bicinchoninic assay and mixed with a Laemmli sample buffer. Proteins were separated by SDS-PAGE and immobilized on PVDF membranes. Membranes were subsequently blocked in 5% (w/v) nonfat dry milk in 50 mM Tris-HCl, pH 7.4, 150 mM NaCl (TBS) plus 0.1% Tween-20 (TBS-Tween), and then incubated overnight (at 4 °C) with the appropriate primary antibody. The next day, membranes were washed in TBS-Tween (3 × 5 min) and incubated with an appropriate IgG HRP-conjugated secondary antibody for 1 h at room temperature. Finally, membranes were washed in TBS-Tween (3 × 5 min), and proteins were revealed using a chemiluminescence reaction (Amersham ECL reagent, GE Healthcare, Chicago, IL). Images were captured using an iBright CL1500 image analysis system (Thermo Fisher Scientific). Primary antibodies: VCAM-1 (#13662), BiP/GRP78 (#3177), HSP90 (#4877), HSP70 (#4873) and HSP40 (#4871), GAPDH (#5174) α-Tubulin (#2125) were from Cell Signaling Technology Inc. (Danvers, MA). ICAM-1/CD54 (sc-8439) and MDR1/ABCB1 (sc-55510) were from Santa Cruz Biotechnology Inc. (Dallas, TX), and anticalreti-

https://doi.org/10.1021/acsptsci.4c00049
ACS Pharmacol. Transl. Sci. 2024, 7, 1823−1838

culin (ab92516) was from Abcam (USA). Secondary antibodies were from Cell Signaling Technology Inc.: antirabbit (#7074) and antimouse (#7076). Expression of VEGFA in the cell culture medium was analyzed by ELISA using reagents from Thermo Fisher Scientific (#BMS277−2).

Secretome Profiling of Human Chemokines. Human SF-268 glioblastoma cells were seeded into 96-well plates, as described above. The next day, seeding medium was replaced with complete medium containing test compounds or vehicle, and plates were returned to the incubator for 24 h. At the end of treatment, the cell culture medium in all wells was replaced with serum-free medium only. After 24 h, the conditioned medium was harvested and concentrated (Thermo Fisher, catalog no. 88515) by centrifugation for 75 min at 4000*g*. Supernatants were flash-frozen with liquid nitrogen and submitted to Eve Technologies Corp., Calgary, Canada, for independent testing against a Human Cytokine/Chemokine Panel A 48-Plex Discovery Array. Forty-three proteins were quantified (Table S1) and five proteins (MIP-1b, IL-12p70, IL-3, IFN-a2, and EGF) were omitted from the analysis because their contents were below the level of detection. SPs, presented in Table S1, were identified through the Uniprot protein database.

Data Analysis. Concentration−response relationships were analyzed, and IC_{50} (Sec61 substrate inhibition) or CC_{50} (cell viability) values determined by nonlinear regression analysis fit to a logistic equation using GraphPad Prism Software version 10.0.02 (GraphPad Software Inc. San Diego, CA). For immunoblot analysis, signals were normalized to the intensity of control proteins (α-tubulin or GAPDH) and quantified with respect to control using an ImageJ software (rsbweb.nih.gov/ij). Heatmaps were created based on the CC_{50} value for each GSC type and ranked for each compound from most resistant (blue) to most potent (red) using a color gradient scheme in a GraphPad Prism software. Statistical significance of the data derived from cell viability assays and quantification of immunoblot assay were performed using one-way analysis of variance (ANOVA) followed by a Student's *t*-test comparing untreated controls and treatment groups. *P*-lower than 0.05 were considered significant.

■ ASSOCIATED CONTENT

Supporting Information

The Supporting Information is available free of charge at https://pubs.acs.org/doi/10.1021/acsptsci.4c00049.

> Experimental procedures, analytical data for synthetic compounds 4 and 5, characteristics of patient-derived glioma stem-like cells (GSCs), and biological data, including details of proteins quantified in the cell secretome (PDF)

■ AUTHOR INFORMATION

Corresponding Authors

Christian E. Badr − *Department of Neurology, Massachusetts General Hospital, Harvard Medical School, Boston, Massachusetts 02129, United States;* orcid.org/0000-0002-7212-5975; Email: badr.christian@mgh.harvard.edu

Jane E. Ishmael − *Department of Pharmaceutical Sciences, College of Pharmacy, Oregon State University, Corvallis, Oregon 97331, United States;* orcid.org/0000-0003-4574-2801; Email: jane.ishmael@oregonstate.edu

Authors

Daphne R. Mattos − *Department of Pharmaceutical Sciences, College of Pharmacy, Oregon State University, Corvallis, Oregon 97331, United States*

Willian das Neves − *Department of Neurology, Massachusetts General Hospital, Harvard Medical School, Boston, Massachusetts 02129, United States*

Takashi Kitamura − *Graduate School of Pharmaceutical Sciences, Kyoto University, Sakyo-ku, Kyoto 606-8501, Japan*

Richa Pradhan − *Department of Neurology, Massachusetts General Hospital, Harvard Medical School, Boston, Massachusetts 02129, United States*

Xuemei Wan − *Department of Pharmaceutical Sciences, College of Pharmacy, Oregon State University, Corvallis, Oregon 97331, United States*

Cintia Carla da Hora − *Department of Neurology, Massachusetts General Hospital, Harvard Medical School, Boston, Massachusetts 02129, United States*

Dale Tranter − *Institute of Biotechnology, University of Helsinki, Helsinki 00014, Finland;* orcid.org/0000-0001-7757-5484

Soheila Kazemi − *Department of Pharmaceutical Sciences, College of Pharmacy, Oregon State University, Corvallis, Oregon 97331, United States*

Xinhui Yu − *Department of Pharmaceutical Sciences, College of Pharmacy, Oregon State University, Corvallis, Oregon 97331, United States*

Nirmalya Tripathy − *Department of Pharmaceutical Sciences, College of Pharmacy, Oregon State University, Corvallis, Oregon 97331, United States;* orcid.org/0000-0003-0439-3908

Ville O. Paavilainen − *Institute of Biotechnology, University of Helsinki, Helsinki 00014, Finland;* orcid.org/0000-0002-3160-7767

Kerry L. McPhail − *Department of Pharmaceutical Sciences, College of Pharmacy, Oregon State University, Corvallis, Oregon 97331, United States;* orcid.org/0000-0003-2076-1002

Shinya Oishi − *Graduate School of Pharmaceutical Sciences, Kyoto University, Sakyo-ku, Kyoto 606-8501, Japan; Laboratory of Medicinal Chemistry, Kyoto Pharmaceutical University, Yamashina-ku, Kyoto 607-8412, Japan;* orcid.org/0000-0002-2833-2539

Complete contact information is available at: https://pubs.acs.org/10.1021/acsptsci.4c00049

Author Contributions

D.R.M., W.N., R.P., X.W., C.C.H., D.T., S.K., N.T., V.O.P., C.E.B., and J.E.I. designed and/or conducted the experiments. T.K., X.Y., K.L.M., and S.O. designed, generated, and/or analyzed all synthetic coibamide compounds. D.R.M., W.N., D.T., S.K., V.O.P., C.E.B., and J.E.I. analyzed all results and interpreted the data. D.R.M. and J.E.I. wrote the first draft of the manuscript. All authors reviewed and edited the final version of the manuscript.

Notes

The authors declare no competing financial interest.

■ ACKNOWLEDGMENTS

This work was supported by grants from the National Institutes of Health: NINDS R21NS119959 (J.E.I., C.E.B.), NINDS R01NS113822 (C.E.B.), NIGMS R01GM132649

(J.E.I., K.L.M., S.O., V.O.P.), and NCCIH T32AT010131 (support of D.R.M.), the Academy of Finland (338836 and 314672) and Sigrid Juselius Foundation (V.O.P.) and the Takeda Science Foundation (S.O.). Some illustrations were created using templates from BioRender. We also thank Oregon State University (OSU) College of Pharmacy for their support of the OSU High-Throughput Screening Services Laboratory.

■ ABBREVIATIONS

BiP, immunoglobulin heavy chain binding protein; CHOP, C/EBP-homologous protein; EGFR, endothelial growth factor receptor; ELISA, enzyme-linked immunosorbent assay; GADD34, growth arrest and DNA damage-inducible protein 34; GRP78, glucose-regulated protein of 78 kDa; Hiv, 2-hydroxyisovaleric acid; ICAM1, intercellular adhesion molecule 1; IL-2, interleukin-2; IL-7, interleukin-7; IRE1, inositol-requiring protein 1; PDFGR, platelet-derived growth factor receptor; sXBP1, spliced X box-binding protein 1; TCGA, The Cancer Genome Atlas; TNFα, tumor necrosis factor alpha; VCAM1, vascular cell adhesion molecule 1; VEGF-A, vascular endothelial growth factor A; VEGFR, vascular endothelial growth factor receptor

■ REFERENCES

(1) Medina, R. A.; Goeger, D. E.; Hills, P.; Mooberry, S. L.; Huang, N.; Romero, L. I.; Ortega-Barria, E.; Gerwick, W. H.; McPhail, K. L. Coibamide, A, a potent antiproliferative cyclic depsipeptide from the Panamanian marine cyanobacterium Leptolyngbya sp. *J. Am. Chem. Soc.* **2008**, *130* (20), 6324−6325.
(2) Luesch, H.; Paavilainen, V. O. Natural products as modulators of eukaryotic protein secretion. *Nat. Prod. Rep.* **2020**, *37* (5), 717−736.
(3) Tranter, D.; Paatero, A. O.; Kawaguchi, S.; Kazemi, S.; Serrill, J. D.; Kellosalo, J.; Vogel, W. K.; Richter, U.; Mattos, D. R.; Wan, X.; Thornburg, C. C.; Oishi, S.; McPhail, K. L.; Ishmael, J. E.; Paavilainen, V. O. Coibamide A Targets Sec61 to Prevent Biogenesis of Secretory and Membrane Proteins. *ACS Chem. Biol.* **2020**, *15* (8), 2125−2136.
(4) Park, E.; Rapoport, T. A. Mechanisms of Sec61/SecY-mediated protein translocation across membranes. *Annu. Rev. Biophys.* **2012**, *41*, 21−40.
(5) Voorhees, R. M.; Hegde, R. S. Structure of the Sec61 channel opened by a signal sequence. *Science* **2016**, *351* (6268), 88−91.
(6) Lang, S.; Pfeffer, S.; Lee, P. H.; Cavalie, A.; Helms, V.; Forster, F.; Zimmermann, R. An Update on Sec61 Channel Functions, Mechanisms, and Related Diseases. *Front. Physiol.* **2017**, *8*, 887.
(7) Rapoport, T. A.; Li, L.; Park, E. Structural and Mechanistic Insights into Protein Translocation. *Annu. Rev. Cell Dev. Biol.* **2017**, *33*, 369−390.
(8) Pool, M. R. Targeting of Proteins for Translocation at the Endoplasmic Reticulum. *Int. J. Mol. Sci.* **2022**, *23* (7), 3773.
(9) Keenan, R. J.; Freymann, D. M.; Stroud, R. M.; Walter, P. The signal recognition particle. *Annu. Rev. Biochem.* **2001**, *70*, 755−775.
(10) Gorlich, D.; Rapoport, T. A. Protein translocation into proteoliposomes reconstituted from purified components of the endoplasmic reticulum membrane. *Cell* **1993**, *75* (4), 615−630.
(11) Van den Berg, B.; Clemons, W. M., Jr.; Collinson, I.; Modis, Y.; Hartmann, E.; Harrison, S. C.; Rapoport, T. A. X-ray structure of a protein-conducting channel. *Nature* **2004**, *427* (6969), 36−44.
(12) Rehan, S.; Tranter, D.; Sharp, P. P.; Craven, G. B.; Lowe, E.; Anderl, J. L.; Muchamuel, T.; Abrishami, V.; Kuivanen, S.; Wenzell, N. A.; Jennings, A.; Kalyanaraman, C.; Strandin, T.; Javanainen, M.; Vapalahti, O.; Jacobson, M. P.; McMinn, D.; Kirk, C. J.; Huiskonen, J. T.; Taunton, J.; Paavilainen, V. O. Signal peptide mimicry primes Sec61 for client-selective inhibition. *Nat. Chem. Biol.* **2023**, *19*, 1054−1062.
(13) Itskanov, S.; Park, E. Mechanism of Protein Translocation by the Sec61 Translocon Complex. *Cold Spring Harbor Perspect. Biol.* **2023**, *15* (1), a041250.
(14) Pauwels, E.; Schulein, R.; Vermeire, K. Inhibitors of the Sec61 Complex and Novel High Throughput Screening Strategies to Target the Protein Translocation Pathway. *Int. J. Mol. Sci.* **2021**, *22* (21), 12007.
(15) Besemer, J.; Harant, H.; Wang, S.; Oberhauser, B.; Marquardt, K.; Foster, C. A.; Schreiner, E. P.; de Vries, J. E.; Dascher-Nadel, C.; Lindley, I. J. Selective inhibition of cotranslational translocation of vascular cell adhesion molecule 1. *Nature* **2005**, *436* (7048), 290−293.
(16) Garrison, J. L.; Kunkel, E. J.; Hegde, R. S.; Taunton, J. A substrate-specific inhibitor of protein translocation into the endoplasmic reticulum. *Nature* **2005**, *436* (7048), 285−289.
(17) Paatero, A. O.; Kellosalo, J.; Dunyak, B. M.; Almaliti, J.; Gestwicki, J. E.; Gerwick, W. H.; Taunton, J.; Paavilainen, V. O. Apratoxin Kills Cells by Direct Blockade of the Sec61 Protein Translocation Channel. *Cell Chem. Biol.* **2016**, *23* (5), 561−566.
(18) Itskanov, S.; Wang, L.; Junne, T.; Sherriff, R.; Xiao, L.; Blanchard, N.; Shi, W. Q.; Forsyth, C.; Hoepfner, D.; Spiess, M.; Park, E. A common mechanism of Sec61 translocon inhibition by small molecules. *Nat. Chem. Biol.* **2023**, *19*, 1063−1071.
(19) Junne, T.; Wong, J.; Studer, C.; Aust, T.; Bauer, B. W.; Beibel, M.; Bhullar, B.; Bruccoleri, R.; Eichenberger, J.; Estoppey, D.; Hartmann, N.; Knapp, B.; Krastel, P.; Melin, N.; Oakeley, E. J.; Oberer, L.; Riedl, R.; Roma, G.; Schuierer, S.; Petersen, F.; Tallarico, J. A.; Rapoport, T. A.; Spiess, M.; Hoepfner, D. Decatransin, a novel natural product inhibiting protein translocation at the Sec61/SecY translocon. *J. Cell Sci.* **2015**, *128* (6), 1217−1229.
(20) Baron, L.; Paatero, A. O.; Morel, J. D.; Impens, F.; Guenin-Mace, L.; Saint-Auret, S.; Blanchard, N.; Dillmann, R.; Niang, F.; Pellegrini, S.; Taunton, J.; Paavilainen, V. O.; Demangel, C. Mycolactone subverts immunity by selectively blocking the Sec61 translocon. *J. Exp. Med.* **2016**, *213* (13), 2885−2896.
(21) Zong, G.; Hu, Z.; O'Keefe, S.; Tranter, D.; Iannotti, M. J.; Baron, L.; Hall, B.; Corfield, K.; Paatero, A. O.; Henderson, M. J.; Roboti, P.; Zhou, J.; Sun, X.; Govindarajan, M.; Rohde, J. M.; Blanchard, N.; Simmonds, R.; Inglese, J.; Du, Y.; Demangel, C.; High, S.; Paavilainen, V. O.; Shi, W. Q. Ipomoeassin F Binds Sec61α to Inhibit Protein Translocation. *J. Am. Chem. Soc.* **2019**, *141* (21), 8450−8461.
(22) Hommel, U.; Weber, H. P.; Oberer, L.; Ulrich Naegeli, H.; Oberhauser, B.; Foster, C. A. The 3D-structure of a natural inhibitor of cell adhesion molecule expression. *FEBS Lett.* **1996**, *379* (1), 69−73.
(23) Chen, Y.; Bilban, M.; Foster, C. A.; Boger, D. L. Solution-phase parallel synthesis of a pharmacophore library of HUN-7293 analogues: a general chemical mutagenesis approach to defining structure-function properties of naturally occurring cyclic (depsi)-peptides. *J. Am. Chem. Soc.* **2002**, *124* (19), 5431−5440.
(24) Schreiner, E. P.; Kern, M.; Steck, A.; Foster, C. A. Synthesis of ether analogues derived from HUN-7293 and evaluation as inhibitors of VCAM-1 expression. *Bioorg. Med. Chem. Lett.* **2004**, *14* (19), 5003−5006.
(25) Maifeld, S. V.; MacKinnon, A. L.; Garrison, J. L.; Sharma, A.; Kunkel, E. J.; Hegde, R. S.; Taunton, J. Secretory Protein Profiling Reveals TNF-α Inactivation by Selective and Promiscuous Sec61 Modulators. *Chem. Biol.* **2011**, *18* (9), 1082−1088.
(26) Harant, H.; Wolff, B.; Schreiner, E. P.; Oberhauser, B.; Hofer, L.; Lettner, N.; Maier, S.; de Vries, J. E.; Lindley, I. J. Inhibition of vascular endothelial growth factor cotranslational translocation by the cyclopeptolide CAM741. *Mol. Pharmacol.* **2007**, *71* (6), 1657−1665.
(27) Vermeire, K.; Bell, T. W.; Van Puyenbroeck, V.; Giraut, A.; Noppen, S.; Liekens, S.; Schols, D.; Hartmann, E.; Kalies, K. U.; Marsh, M. Signal peptide-binding drug as a selective inhibitor of co-translational protein translocation. *PLoS Biol.* **2014**, *12* (12), No. e1002011.

https://doi.org/10.1021/acsptsci.4c00049
ACS Pharmacol. Transl. Sci. 2024, 7, 1823−1838

(28) Klein, W.; Westendorf, C.; Schmidt, A.; Conill-Cortes, M.; Rutz, C.; Blohs, M.; Beyermann, M.; Protze, J.; Krause, G.; Krause, E.; Schulein, R. Defining a conformational consensus motif in cotransin-sensitive signal sequences: a proteomic and site-directed mutagenesis study. *PLoS One* **2015**, *10* (3), No. e0120886.
(29) Sicking, M.; Lang, S.; Bochen, F.; Roos, A.; Drenth, J. P. H.; Zakaria, M.; Zimmermann, R.; Linxweiler, M. Complexity and Specificity of Sec61-Channelopathies: Human Diseases Affecting Gating of the Sec61 Complex. *Cells* **2021**, *10* (5), 1036.
(30) Luesch, H.; Chanda, S. K.; Raya, R. M.; DeJesus, P. D.; Orth, A. P.; Walker, J. R.; Izpisua Belmonte, J. C.; Schultz, P. G. A functional genomics approach to the mode of action of apratoxin A. *Nat. Chem. Biol.* **2006**, *2* (3), 158−167.
(31) Ruiz-Saenz, A.; Sandhu, M.; Carrasco, Y.; Maglathlin, R. L.; Taunton, J.; Moasser, M. M. Targeting HER3 by interfering with its Sec61-mediated cotranslational insertion into the endoplasmic reticulum. *Oncogene* **2015**, *34* (41), 5288−5294.
(32) Huang, K. C.; Chen, Z. H.; Jiang, Y. M.; Akare, S.; Kolber-Simonds, D.; Condon, K.; Agoulnik, S.; Tendyke, K.; Shen, Y. C.; Wu, K. M.; Mathieu, S.; Choi, H. W.; Zhu, X. J.; Shimizu, H.; Kotake, Y.; Gerwick, W. H.; Uenaka, T.; Woodall-Jappe, M.; Nomoto, K. Apratoxin A Shows Novel Pancreas-Targeting Activity through the Binding of Sec 61. *Mol. Cancer Ther.* **2016**, *15* (6), 1208−1216.
(33) Serrill, J. D.; Wan, X.; Hau, A. M.; Jang, H. S.; Coleman, D. J.; Indra, A. K.; Alani, A. W.; McPhail, K. L.; Ishmael, J. E. Coibamide A, a natural lariat depsipeptide, inhibits VEGFA/VEGFR2 expression and suppresses tumor growth in glioblastoma xenografts. *Invest. New Drugs* **2016**, *34* (1), 24−40.
(34) Lowe, E.; Fan, R. A.; Jiang, J.; Johnson, H. W. B.; Kirk, C. J.; McMinn, D.; Millare, B.; Muchamuel, T.; Qian, Y.; Tuch, B. B.; Whang, J. A.; Zuno, P. Preclinical evaluation of KZR-261, a novel small molecule inhibitor of Sec61. *J. Clin. Oncol.* **2020**, *38* (15_suppl), 3582.
(35) Domenger, A.; Choisy, C.; Baron, L.; Mayau, V.; Perthame, E.; Deriano, L.; Arnulf, B.; Bories, J. C.; Dadaglio, G.; Demangel, C. The Sec61 translocon is a therapeutic vulnerability in multiple myeloma. *EMBO Mol. Med.* **2022**, *14* (3), No. e14740.
(36) Hau, A. M.; Greenwood, J. A.; Lohr, C. V.; Serrill, J. D.; Proteau, P. J.; Ganley, I. G.; McPhail, K. L.; Ishmael, J. E. Coibamide A induces mTOR-independent autophagy and cell death in human glioblastoma cells. *PLoS One* **2013**, *8* (6), No. e65250.
(37) Kazemi, S.; Kawaguchi, S.; Badr, C. E.; Mattos, D. R.; Ruiz-Saenz, A.; Serrill, J. D.; Moasser, M. M.; Dolan, B. P.; Paavilainen, V. O.; Oishi, S.; McPhail, K. L.; Ishmael, J. E. Targeting of HER/ErbB family proteins using broad spectrum Sec61 inhibitors coibamide A and apratoxin A. *Biochem. Pharmacol.* **2021**, *183*, 114317.
(38) Shi, W.; Lu, D.; Wu, C.; Li, M.; Ding, Z.; Li, Y.; Chen, B.; Lin, X.; Su, W.; Shao, X.; Xia, Z.; Fang, L.; Liu, K.; Li, H. Coibamide A kills cancer cells through inhibiting autophagy. *Biochem. Biophys. Res. Commun.* **2021**, *547*, 52−58.
(39) Wan, X.; Serrill, J. D.; Humphreys, I. R.; Tan, M.; McPhail, K. L.; Ganley, I. G.; Ishmael, J. E. ATG5 Promotes Death Signaling in Response to the Cyclic Depsipeptides Coibamide A and Apratoxin A. *Mar. Drugs* **2018**, *16* (3), 77.
(40) Yao, G.; Wang, W.; Ao, L.; Cheng, Z.; Wu, C.; Pan, Z.; Liu, K.; Li, H.; Su, W.; Fang, L. Improved Total Synthesis and Biological Evaluation of Coibamide A Analogues. *J. Med. Chem.* **2018**, *61* (19), 8908−8916.
(41) Kitamura, T.; Suzuki, R.; Inuki, S.; Ohno, H.; McPhail, K. L.; Oishi, S. Design of Coibamide A Mimetics with Improved Cellular Bioactivity. *ACS Med. Chem. Lett.* **2022**, *13* (1), 105−110.
(42) Gerard, S. F.; Hall, B. S.; Zaki, A. M.; Corfield, K. A.; Mayerhofer, P. U.; Costa, C.; Whelligan, D. K.; Biggin, P. C.; Simmonds, R. E.; Higgins, M. K. Structure of the Inhibited State of the Sec Translocon. *Mol. Cell* **2020**, *79* (3), 406−415.e7.
(43) Cai, W.; Ratnayake, R.; Wang, M.; Chen, Q. Y.; Raisch, K. P.; Dang, L. H.; Law, B. K.; Luesch, H. Inhibition of cotranslational translocation by apratoxin S4: Effects on oncogenic receptor tyrosine kinases and the fate of transmembrane proteins produced in the cytoplasm. *Curr. Res. Pharmacol. Drug Discov.* **2021**, *2*, 100053.
(44) Mattos, D. R.; Weinman, M. A.; Wan, X.; Goodall, C. P.; Serrill, J. D.; McPhail, K. L.; Milovancev, M.; Bracha, S.; Ishmael, J. E. Canine osteosarcoma cells exhibit basal accumulation of multiple chaperone proteins and are sensitive to small molecule inhibitors of GRP78 and heat shock protein function. *Cell Stress Chaperones* **2022**, *27*, 223−239.
(45) Kelly, C. N.; Townsend, C. E.; Jain, A. N.; Naylor, M. R.; Pye, C. R.; Schwochert, J.; Lokey, R. S. Geometrically Diverse Lariat Peptide Scaffolds Reveal an Untapped Chemical Space of High Membrane Permeability. *J. Am. Chem. Soc.* **2021**, *143* (2), 705−714.
(46) He, W.; Qiu, H. B.; Chen, Y. J.; Xi, J.; Yao, Z. J. Total synthesis of proposed structure of coibamide A, a highly N- and O-methylated cytotoxic marine cyclodepsipeptide. *Tetrahedron Lett.* **2014**, *55* (44), 6109−6112.
(47) Nabika, R.; Suyama, T. L.; Hau, A. M.; Misu, R.; Ohno, H.; Ishmael, J. E.; McPhail, K. L.; Oishi, S.; Fujii, N. Synthesis and biological evaluation of the [d-MeAla(11)]-epimer of coibamide A. *Bioorg. Med. Chem. Lett.* **2015**, *25* (2), 302−306.
(48) Yao, G.; Pan, Z.; Wu, C.; Wang, W.; Fang, L.; Su, W. Efficient Synthesis and Stereochemical Revision of Coibamide A. *J. Am. Chem. Soc.* **2015**, *137* (42), 13488−13491.
(49) Lukas, R. V.; Wainwright, D. A.; Ladomersky, E.; Sachdev, S.; Sonabend, A. M.; Stupp, R. Newly Diagnosed Glioblastoma: A Review on Clinical Management. *Oncology (Williston Park)* **2019**, *33* (3), 91−100.
(50) Lu, Z.; Zhou, L.; Killela, P.; Rasheed, A. B.; Di, C.; Poe, W. E.; McLendon, R. E.; Bigner, D. D.; Nicchitta, C.; Yan, H. Glioblastoma Proto-oncogene SEC61γ Is Required for Tumor Cell Survival and Response to Endoplasmic Reticulum Stress. *Cancer Res.* **2009**, *69* (23), 9105−9111.
(51) Johnson, G. G.; White, M. C.; Wu, J. H.; Vallejo, M.; Grimaldi, M. The deadly connection between endoplasmic reticulum, Ca2+, protein synthesis, and the endoplasmic reticulum stress response in malignant glioma cells. *Neuro Oncol.* **2014**, *16* (8), 1086−1099.
(52) Gao, H.; Niu, W.; He, Z.; Gao, C.; Peng, C.; Niu, J. SEC61G plays an oncogenic role in hepatocellular carcinoma cells. *Cell Cycle* **2020**, *19* (23), 3348−3361.
(53) Ma, J.; He, Z.; Zhang, H.; Zhang, W.; Gao, S.; Ni, X. SEC61G promotes breast cancer development and metastasis via modulating glycolysis and is transcriptionally regulated by E2F1. *Cell Death Dis.* **2021**, *12* (6), 550.
(54) Zheng, Q.; Wang, Z.; Zhang, M.; Yu, Y.; Chen, R.; Lu, T.; Liu, L.; Ma, J.; Liu, T.; Zheng, H.; Li, H.; Li, J. Prognostic value of SEC61G in lung adenocarcinoma: a comprehensive study based on bioinformatics and in vitro validation. *BMC Cancer* **2021**, *21* (1), 1216.
(55) Lu, T.; Chen, Y.; Gong, X.; Guo, Q.; Lin, C.; Luo, Q.; Tu, Z.; Pan, J.; Li, J. SEC61G overexpression and DNA amplification correlates with prognosis and immune cell infiltration in head and neck squamous cell carcinoma. *Cancer Med.* **2021**, *10* (21), 7847−7862.
(56) Liu, B.; Liu, J.; Liao, Y.; Jin, C.; Zhang, Z.; Zhao, J.; Liu, K.; Huang, H.; Cao, H.; Cheng, Q. Identification of SEC61G as a Novel Prognostic Marker for Predicting Survival and Response to Therapies in Patients with Glioblastoma. *Med. Sci. Monit* **2019**, *25*, 3624−3635.
(57) Lathia, J. D.; Mack, S. C.; Mulkearns-Hubert, E. E.; Valentim, C. L.; Rich, J. N. Cancer stem cells in glioblastoma. *Genes Dev.* **2015**, *29* (12), 1203−1217.
(58) da Hora, C. C.; Schweiger, M. W.; Wurdinger, T.; Tannous, B. A. Patient-Derived Glioma Models: From Patients to Dish to Animals. *Cells* **2019**, *8* (10), 1177.
(59) Ron, D.; Walter, P. Signal integration in the endoplasmic reticulum unfolded protein response. *Nat. Rev. Mol. Cell Biol.* **2007**, *8* (7), 519−529.
(60) Schroder, M.; Kaufman, R. J. The mammalian unfolded protein response. *Annu. Rev. Biochem.* **2005**, *74*, 739−789.

(61) Kosakowska-Cholody, T.; Lin, J.; Srideshikan, S. M.; Scheffer, L.; Tarasova, N. I.; Acharya, J. K. HKH40A downregulates GRP78/BiP expression in cancer cells. *Cell Death Dis.* **2014**, *5* (5), No. e1240.
(62) Cerezo, M.; Lehraiki, A.; Millet, A.; Rouaud, F.; Plaisant, M.; Jaune, E.; Botton, T.; Ronco, C.; Abbe, P.; Amdouni, H.; Passeron, T.; Hofman, V.; Mograbi, B.; Dabert-Gay, A. S.; Debayle, D.; Alcor, D.; Rabhi, N.; Annicotte, J. S.; Heliot, L.; Gonzalez-Pisfil, M.; Robert, C.; Morera, S.; Vigouroux, A.; Gual, P.; Ali, M. M. U.; Bertolotto, C.; Hofman, P.; Ballotti, R.; Benhida, R.; Rocchi, S. Compounds Triggering ER Stress Exert Anti-Melanoma Effects and Overcome BRAF Inhibitor Resistance. *Cancer Cell* **2016**, *30* (1), 183.
(63) Snyder, K. M.; Sikorska, J.; Ye, T.; Fang, L.; Su, W.; Carter, R. G.; McPhail, K. L.; Cheong, P. H. Towards theory driven structure elucidation of complex natural products: mandelalides and coibamide A. *Org. Biomol. Chem.* **2016**, *14* (24), 5826−5831.
(64) Tannous, B. A.; Kim, D. E.; Fernandez, J. L.; Weissleder, R.; Breakefield, X. O. Codon-optimized Gaussia luciferase cDNA for mammalian gene expression in culture and in vivo. *Mol. Ther.* **2005**, *11* (3), 435−443.
(65) Serrill, J. D.; Tan, M.; Fotso, S.; Sikorska, J.; Kasanah, N.; Hau, A. M.; McPhail, K. L.; Santosa, D. A.; Zabriskie, T. M.; Mahmud, T.; Viollet, B.; Proteau, P. J.; Ishmael, J. E. Apoptolidins A and C activate AMPK in metabolically sensitive cell types and are mechanistically distinct from oligomycin A. *Biochem. Pharmacol.* **2015**, *93* (3), 251−265.
(66) Smalinskaite, L.; Kim, M. K.; Lewis, A. J. O.; Keenan, R. J.; Hegde, R. S. Mechanism of an intramembrane chaperone for multipass membrane proteins. *Nature* **2022**, *611* (7934), 161−166.
(67) Sundaram, A.; Yamsek, M.; Zhong, F.; Hooda, Y.; Hegde, R. S.; Keenan, R. J. Substrate-driven assembly of a translocon for multipass membrane proteins. *Nature* **2022**, *611* (7934), 167−172.
(68) Morel, J. D.; Paatero, A. O.; Wei, J.; Yewdell, J. W.; Guenin-Mace, L.; Van Haver, D.; Impens, F.; Pietrosemoli, N.; Paavilainen, V. O.; Demangel, C. Proteomics Reveals Scope of Mycolactone-mediated Sec61 Blockade and Distinctive Stress Signature. *Mol. Cell. Proteomics* **2018**, *17* (9), 1750−1765.
(69) Verhaak, R. G.; Hoadley, K. A.; Purdom, E.; Wang, V.; Qi, Y.; Wilkerson, M. D.; Miller, C. R.; Ding, L.; Golub, T.; Mesirov, J. P.; Alexe, G.; Lawrence, M.; O'Kelly, M.; Tamayo, P.; Weir, B. A.; Gabriel, S.; Winckler, W.; Gupta, S.; Jakkula, L.; Feiler, H. S.; Hodgson, J. G.; James, C. D.; Sarkaria, J. N.; Brennan, C.; Kahn, A.; Spellman, P. T.; Wilson, R. K.; Speed, T. P.; Gray, J. W.; Meyerson, M.; Getz, G.; Perou, C. M.; Hayes, D. N. Integrated Genomic Analysis Identifies Clinically Relevant Subtypes of Glioblastoma Characterized by Abnormalities in PDGFRA, IDH1, EGFR, and NF1. *Cancer Cell* **2010**, *17* (1), 98−110.
(70) Nakano, I. Stem cell signature in glioblastoma: therapeutic development for a moving target. *J. Neurosurg.* **2015**, *122* (2), 324−330.
(71) Ceccarelli, M.; Barthel, F. P.; Malta, T. M.; Sabedot, T. S.; Salama, S. R.; Murray, B. A.; Morozova, O.; Newton, Y.; Radenbaugh, A.; Pagnotta, S. M.; Anjum, S.; Wang, J.; Manyam, G.; Zoppoli, P.; Ling, S.; Rao, A. A.; Grifford, M.; Cherniack, A. D.; Zhang, H.; Poisson, L.; Carlotti, C. G., Jr.; Tirapelli, D. P.; Rao, A.; Mikkelsen, T.; Lau, C. C.; Yung, W. K.; Rabadan, R.; Huse, J.; Brat, D. J.; Lehman, N. L.; Barnholtz-Sloan, J. S.; Zheng, S.; Hess, K.; Rao, G.; Meyerson, M.; Beroukhim, R.; Cooper, L.; Akbani, R.; Wrensch, M.; Haussler, D.; Aldape, K. D.; Laird, P. W.; Gutmann, D. H.; Network, T. R.; Noushmehr, H.; Iavarone, A.; Verhaak, R. G. Molecular Profiling Reveals Biologically Discrete Subsets and Pathways of Progression in Diffuse Glioma. *Cell* **2016**, *164* (3), 550−563.
(72) Badr, C. E.; Silver, D. J.; Siebzehnrubl, F. A.; Deleyrolle, L. P. Metabolic heterogeneity and adaptability in brain tumors. *Cell. Mol. Life Sci.* **2020**, *77* (24), 5101−5119.
(73) Zeng, K.; Zeng, Y.; Zhan, H.; Zhan, Z.; Wang, L.; Xie, Y.; Tang, Y.; Li, C.; Chen, Y.; Li, S.; Liu, M.; Chen, X.; Liang, L.; Deng, F.; Song, Y.; Zhou, A. SEC61G assists EGFR-amplified glioblastoma to evade immune elimination. *Proc. Natl. Acad. Sci. U.S.A.* **2023**, *120* (32), No. e2303400120.
(74) Liu, Y.; Law, B. K.; Luesch, H. Apratoxin a reversibly inhibits the secretory pathway by preventing cotranslational translocation. *Mol. Pharmacol.* **2009**, *76* (1), 91−104.
(75) Li, C. W.; Lim, S. O.; Xia, W.; Lee, H. H.; Chan, L. C.; Kuo, C. W.; Khoo, K. H.; Chang, S. S.; Cha, J. H.; Kim, T.; Hsu, J. L.; Wu, Y.; Hsu, J. M.; Yamaguchi, H.; Ding, Q.; Wang, Y.; Yao, J.; Lee, C. C.; Wu, H. J.; Sahin, A. A.; Allison, J. P.; Yu, D.; Hortobagyi, G. N.; Hung, M. C. Glycosylation and stabilization of programmed death ligand-1 suppresses T-cell activity. *Nat. Commun.* **2016**, *7*, 12632.
(76) Xu, Y.; Gao, Z.; Hu, R.; Wang, Y.; Wang, Y.; Su, Z.; Zhang, X.; Yang, J.; Mei, M.; Ren, Y.; Li, M.; Zhou, X. PD-L2 glycosylation promotes immune evasion and predicts anti-EGFR efficacy. *J. Immunother Cancer* **2021**, *9* (10), No. e002699.
(77) Huang, H. J. S.; Nagane, M.; Klingbeil, C. K.; Lin, H.; Nishikawa, R.; Ji, X. D.; Huang, C. M.; Gill, G. N.; Wiley, H. S.; Cavenee, W. K. The enhanced tumorigenic activity of a mutant epidermal growth factor receptor common in human cancers is mediated by threshold levels of constitutive tyrosine phosphorylation and unattenuated signaling. *J. Biol. Chem.* **1997**, *272* (5), 2927−2935.
(78) Gan, H. K.; Cvrljevic, A. N.; Johns, T. G. The epidermal growth factor receptor variant III (EGFRvIII): where wild things are altered. *FEBS J.* **2013**, *280* (21), 5350−5370.
(79) Thornburg, C. C.; Cowley, E. S.; Sikorska, J.; Shaala, L. A.; Ishmael, J. E.; Youssef, D. T.; McPhail, K. L. Apratoxin H and apratoxin A sulfoxide from the Red Sea cyanobacterium Moorea producens. *J. Nat. Prod.* **2013**, *76* (9), 1781−1788.
(80) Eyme, K. M.; Sammarco, A.; Jha, R.; Mnatsakanyan, H.; Pechdimaljian, C.; Carvalho, L.; Neustadt, R.; Moses, C.; Alnasser, A.; Tardiff, D. F.; Su, B.; Williams, K. J.; Bensinger, S. J.; Chung, C. Y.; Badr, C. E. Targeting de novo lipid synthesis induces lipotoxicity and impairs DNA damage repair in glioblastoma mouse models. *Sci. Transl. Med.* **2023**, *15* (679), No. eabq6288.

https://doi.org/10.1021/acsptsci.4c00049
ACS Pharmacol. Transl. Sci. 2024, 7, 1823−1838